CHEMICAL REVIEWS

REVIEW

pubs.acs.org/CR

Confined Nanospaces in Metallocages: Guest Molecules, Weakly Encapsulated Anions, and Catalyst Sequestration

Hani Amouri,* Christophe Desmarets, and Jamal Moussa

Institut Parisien de Chimie Moléculaire, UMR CNRS 7201, Université Pierre et Marie Curie Paris-6, 4 place Jussieu, case 42, 75252 Paris Cedex 05, France

CONTENTS

1. INTRODUCTION

In the past two decades, there has been a great deal of interest in designing metal-based 3D capsules with nanocavities.[1−6] These studies are inspired by the fact that such cavities can be regarded as mimics of the active sites of enzymes, able to perform host−guest recognition, anion sensing, and ultimately even important catalytic transformations in supramolecular media where the proximity of functional groups and substrate preorganization with favorable overlap can lead to catalytic activity surpassing that occurring through conventional means. A number of reviews and papers have been recently published on these topics.[7−9] In contrast, here in this review we highlight (i) the recent contributions devoted to 3D metallocryptands (e.g., **A** in Chart 1) and metallocages for guest molecules (e.g., **C**) and weakly coordinated anions with emphasis on metal−anion interaction (e.g., **B**) that were overlooked in previous reviews.[10] Further the scope of the review will be limited to (ii) nanocavities without a catalyst (e.g., **E** and **F**) that perform some unusual chemical reactions as a result of preorganization of reactive substrates and (iii) supramolecular systems, where catalysts are sequestrated within the cavities of nanocapsules to form nanoreactors (e.g., **F**) that exhibit interesting catalytic properties in supramolecular media.

2. METALLOCRYPTANDS, METALLOMACROCYCLES, METALLOCAGES, METALLOBOXES, AND PRISMS

2.1. General Considerations

Host−guest interactions represent one of the most important aspects of contemporary supramolecular chemistry.[11,12] Traditionally host−guest chemistry was dominated by organic receptors such as crown ethers, cyclophanes, cyclodextrins, calixarenes, and cryptands.[13−15] In fact the term cryptand was coined by Lehn and co-workers in 1969;[16] we note that a related term for an anion receptor *katapinand* was used in the previous year by Simmons and Park.[17,18] This kind of artificial receptor is suitably designed to create a confined space to encapsulate guest molecules and has been widely studied in the literature. Because this review is devoted to assemblies prepared by a coordination chemistry approach, for metal-free anion receptors the reader may consult a recent review on metal-free anion receptors by Bowman-James and co-workers.[19] Starting in the mid-1990s a novel approach based on coordination-driven self-assembly to construct discrete nanoscopic supramolecular species with predetermined shapes, geometries, and symmetries was developed. Directional metal−ligand bonds, a consequence of preferred coordination environments of the metal ions in combination with the appropriate rigid ligand, allow a certain control of the supramolecular architecture, which is thermodynamically more stable than the starting components or any kinetically formed intermediates. The energies of the metal−ligand bonds

Received: August 31, 2011
Published: January 17, 2012

ACS Publications © 2012 American Chemical Society

Chart 1. Examples of 3D Coordination Ensembles (A−F) with Internal Cavities Used As Molecular Flasks

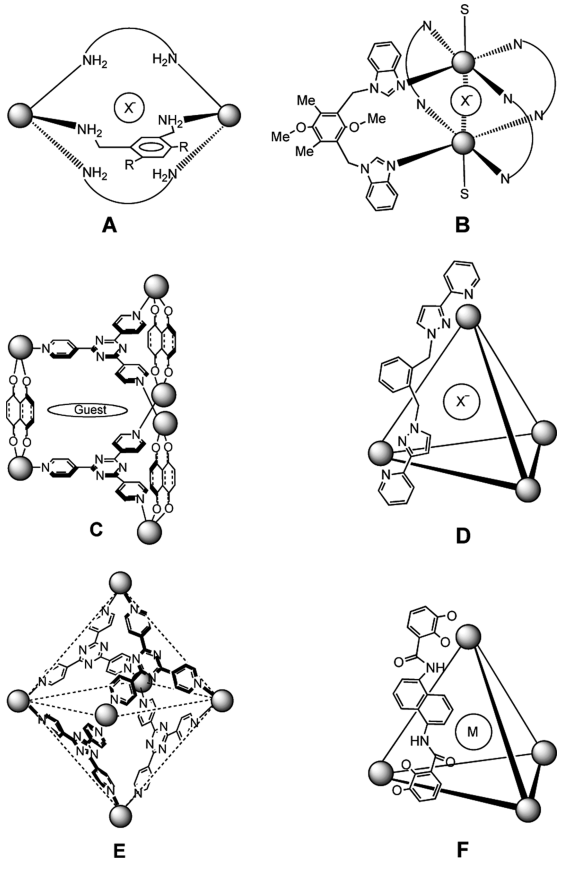

Scheme 1. Metallocryptands and Metallocryptates

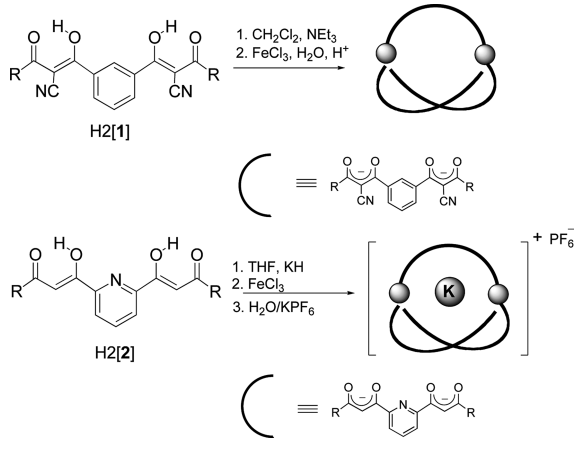

(ca. 15−50 kcal/mol) are weaker than those encountered in covalent organic synthesis (ca. 60−120 kcal/mol).

A wide range of coordination assemblies were prepared including metallomacrocycles, triangles, rectangles, polygons, and in particular metallocryptands and 3D tetrahedral and octahedral nanocages. The latter possesses confined nanospaces that were used for host−guest chemistry and showed unusual reactivity, which in some cases cannot be achieved through classical procedures.

2.2. Metallocryptands

Saalfrank and co-workers reported the synthesis of some chiral metallocyptands of Fe(III) using tailor-made tetradentate ligands with *m*-phenylene H2[**1**] and *m*-pyridylene H2[**2**] spacers (Scheme 1).[20,21] The free-guest metallocryptands $[Fe_2(\mathbf{1})_3]$ and $[Fe_2(\mathbf{2})_3]$ were obtained with (Δ, Δ) or (Λ, Λ) configurations at the metal center and were defined as a *metallotopomers* of 2-cryptands. Interestingly the related helicates $[K\subset(Fe_2(\mathbf{2})_3)][PF_6]$ with a guest cation inside the cavity exhibited achiral meso-configuration (Δ, Λ) at the metal centers. The latter were defined as a *metallotopomers* of 2-cryptates.

Catalano et al. reported the self-assembly of some metallocryptands using phosphinophenanthroline assembling ligands "P2Phen" and Au(I) closed-shell d^{10} bricks in 3/2 ratio (Scheme 2).[22] These cryptands are capable of encapsulating a variety of cations such as Na^+ and K^+ ions and in some cases bromide anions. These host metallocryptands were used to probe closed-shell metal−metal interactions, which in some cases resulted in luminescent metallocryptates.[23]

In 2001 we reported the first example of rhodio- and iridiocryptands and -cryptates based on Cp*M solvated piano stool bricks (M = Rh, Ir) and diamine linkers.[24] The cavity size and shape were easy to modify by simply changing the nature of the bridging diamine ligand. Consequently these metallocryptands **3** and **4** were adequate to encapsulate weakly coordinated BF_4 anions (Scheme 3).[25]

2.3. Metallocages and Metallomacrocycles

Metallocages based on Cp*M molecular bricks have been recently the subject of intensive research activity of many groups.[26,27] For example, Rauchfuss and co-workers reported the synthesis of cubic structures with half-sandwich complexes. By using $[Cp^*Rh(CN)_3]^{-1}$ molecular bricks[28,29] or $[CpCo(CN)_3]^{-1}$[30] as bridging ligand in combination with other metal complexes such as $[(C_6H_3Me_3)Mo(CO)_3]$, $[Cp^*RhCl_2]_2$, $[Cp^*Rh(CH_3CN)_3][PF_6]_2$, and $[Cp^*Ru(CH_3CN)_3][PF_6]$, a variety of cubic metallocages were obtained. These metallocages act as receptors for small cations (Scheme 4).[31,32]

Severin reported the synthesis of a variety of neutral trinuclear metallomacrocycles $[(\eta\text{-ring})ML]_3$ displaying bowl-like shape and with internal cone cavity.[33,34] These metallobowls are efficient hosts for alkali metal ions (Li, Na, and K).[35] The author has also reported that the size of the metallobowl depends on the angle between the two coordination vectors within the organic linkers. When this angle is ∼90°, a trinuclear assembly is obtained. In the case when the coordinate vectors become >90°, the bridging ligand induces formation of much wider angles and the buildup of tetranuclear squares.[36] Moreover Severin and co-workers also constructed a hexanuclear coordination ruthenium cage from the tritopic rigid ligand 2,4,6-tris(pyridin-4yl)-1,3,5-triazine (tpt) and the dinuclear complex $[(p\text{-cymene})Ru(\mu\text{-3,6-dimethoxynaphthalene-2,7-dicarboxylate})]_2$. Interestingly this coordination cage showed flexible cavity modulation up to 500 Å^3 and was capable to encapsulate two molecules of coronene (Figure 1).[37]

More recently, Severin and co-workers described an elegant approach to construct giant molecular cages[38] by connecting the metallomacrocyclic trialdehydes $[(\eta\text{-ring})Ru(4\text{-formyl-3-hydroxy-2-pyridone})]_3$ with tritopic amine ligands (**5**−**7**) via dynamic covalent chemistry (Scheme 5). Indeed a variety of metallocages with 3, 6, and even 12 metal centers were formed successfully as confirmed by their X-ray molecular structures.

Scheme 2. Formation of Gold Cryptates

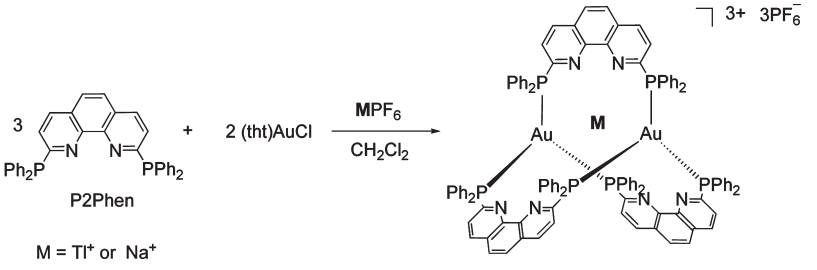

Scheme 3. Synthesis and X-ray Molecular Structure of Iridiocryptand (4)

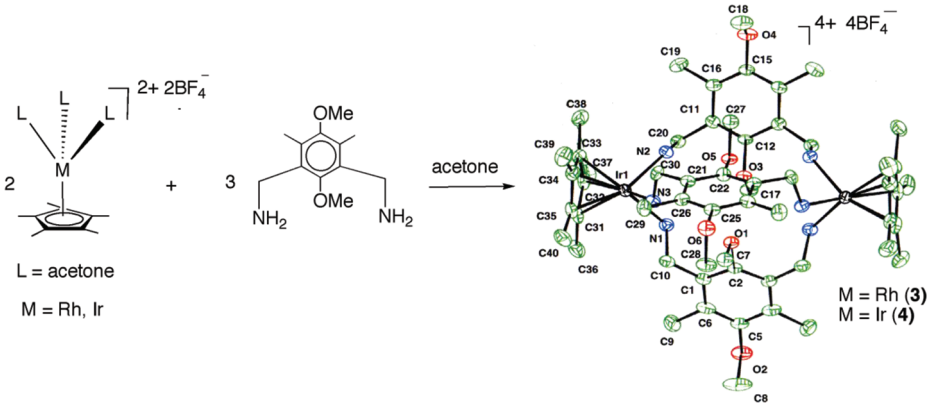

Scheme 4. Cubic Metallocages

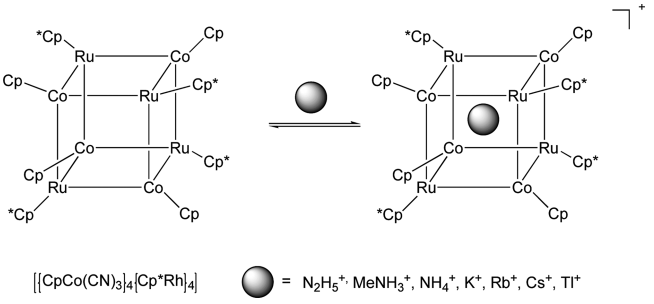

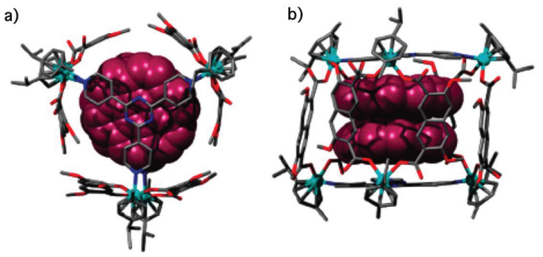

Figure 1. Molecular structure of the hexanuclear ruthenium coordination cage encapsulating two molecules of coronenes: (a) top view and (b) side view. Reprinted with permission from ref 37. Copyright 2010 American Chemical Society.

Remarkably some of the above cages were prepared in one-pot reactions by mixing $[(\text{arene})RuCl_2]_2$ with the pyridone ligand and the amine in the presence of the base. Severin and co-workers have also noticed that the above assemblies proceeded with diastereoselective and chemoselective (self-sorting) fashion.[39]

On the other hand, an important property of the related trinuclear metallomacrocycles $[(\eta\text{-ring})M(L)]_3$ is their chirality (M = Ru, Rh, Ir; H2L = 2,3-dihydroxypyridine). These macrocycles were reported as racemates through homochiral self-assembly (all metals have the same configuration $R_MR_MR_M$/$S_MS_MS_M$). Yamanari and co-workers have reported the separation of the diastereomers of the cationic trinuclear metallomacrocycles $[Cp^*M(ado)]_3[OTf]_3$ (M = Rh, Ir; ado = adenosine) through crystallization,[40] but no NMR studies have been made to differentiate these chiral macrocycles by the use of a chiral auxiliary. Amouri and co-workers reported the synthesis of some neutral rhodium, iridium, and ruthenium trinuclear metallobowls. All attempts to resolve the ruthenium and iridium metallomacrocycles were unsuccessful because anion metathesis with Δ-TRISPHAT did not occur; only the rhodium congeners were amenable to chiral differentiation using Lacour's Δ-TRISPHAT anion {TRISPHAT = tris[tetrachlorobenzene-1,2-bis(olato)]phosphate}.[41] Conversion of the racemic material to a mixture of diastereomeric salts began by encapsulation of a lithium cation. Subsequent anion metathesis using the optically pure chiral shift reagent [Cinchonidinium][Δ-TRISPHAT] provided a pair of diastereomers $[Li\subset(R,R,R)\text{-}\{Cp^*Rh(5\text{-chloro-}2,3\text{-dioxopyridine})\}_3][\Delta\text{-TRISPHAT}]$ (**8a**) and $[Li\subset(S,S,S)\text{-}\{Cp^*Rh(5\text{-chloro-}2,3\text{-dioxopyridine})\}_3][\Delta\text{-TRISPHAT}]$ (**8b**). The latter were separated by fractional crystallization.[42,43]

The X-ray molecular structure of one of the diastereomers with (*R*,*R*,*R*)-configuration is presented in Figure 2. The structure

dx.doi.org/10.1021/cr200345v |*Chem. Rev.* 2012, 112, 2015–2041

Scheme 5. Synthesis of the Tetrahedral Cages

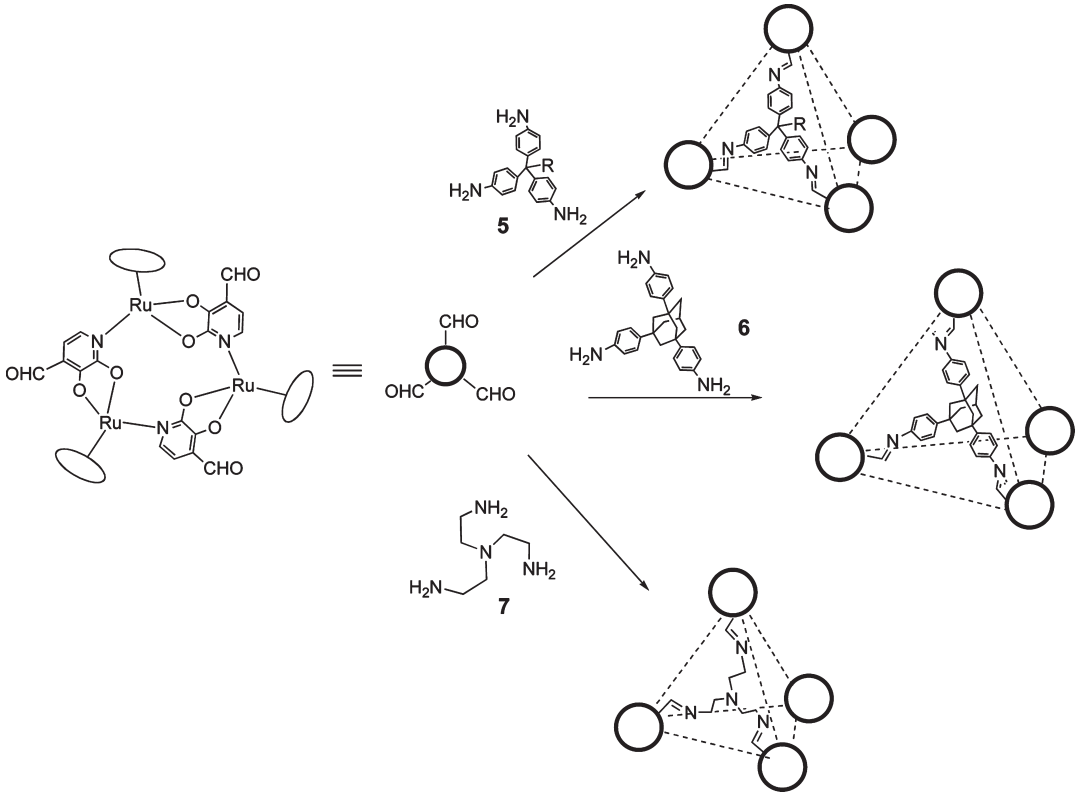

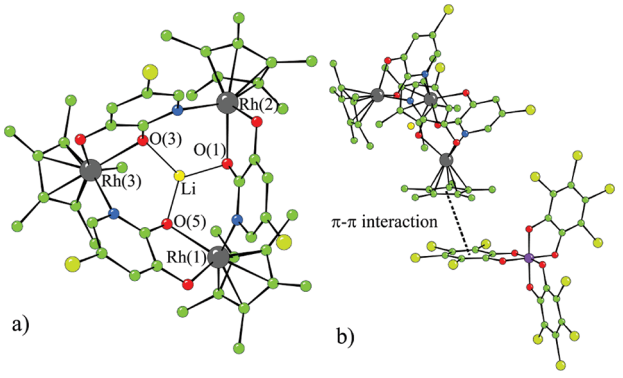

Figure 2. (a) Frontal projection of the cationic part of **8a** showing Li^+ encapsulation with atom numbering system and (b) sidewise projection of **8a** showing the $\pi-\pi$ interaction between Δ-TRISPHAT and triangular host.

provided valuable information about the nature of chiral recognition between the optically pure anion and the cationic complex; this chiral recognition occurs through $\pi-\pi$ interactions as beautifully illustrated in Figure 2b. Circular dichroism (CD) spectra and NMR studies in solution show an enhancement of the configurational stability at the metal centers in the cationic species compared to the starting neutral racemic metallobowl [Cp*Rh-(5-chloro-2,3-dioxopyridine)]$_3$ (**9**) (Figure 3).

2.4. Metalloboxes and Metalloprisms

Therrien and co-workers constructed bimetallic connectors **10** by combining [(arene)Ru(μ-Cl)Cl]$_2$ with dihydroxy 1,4-benzoquinone. By subsequent treatment with tridentate 2,4,6-tris(pyridin-4yl)-1,3,5-triazine (tpt) paneling ligand, a variety of hexanuclear arene ruthenium metallaprisms with large cavities were obtained.[44,45] These cages showed properties as hosts to accommodate planar molecules.[46,47]For example, permanent encapsulation of large aromatic molecules such as pyrene, triphenylene, and coronene has been observed (Scheme 6).[48−50] In these systems the host−guest complexes act as carceplexes. "*A carceplex is an incarcerated host−guest complex where the guest molecule is permanently trapped.*" Furthermore, these organometallic capsules allowed also the encapsulation of the square-planar complexes and were found to act in drug delivery.[51] Indeed, Therrien and co-workers reported recently the encapsulation of pyrenyl-containing dendrimers Pn into water-soluble arene−ruthenium metallaprism (where Pn = P0, P1, and P2 are three generations of cyanobiphenyl dendritic precursors. The host−guest systems [Pn⊂Ru_6(*p*-cymene)$_6$(tpt)$_2$(donq)$_3$][CF_3SO_3]$_6$ (**11**) (donq = 5,8-dioxido-1,4-naphthoquinonato) were found to be remarkably stable in solution. The cytotoxicity of the host−guest system has been evaluated on human ovarien A2780 and A2780cisR cancer cell lines, and an increase of 1 order of magnitude was found when compared with the empty metallaprism.[52] These studies show that metallacage host systems are able to deliver hydrophobic guest molecules with extremely large appendages into cancer cells.

This kind of supramolecular chemistry based on organometallic piano-stool bricks has been also investigated by Jin and co-workers.[6,53,54] Thus, tetranuclear metallorectangles based on Cp*M molecular bricks with modular cavities for host−guest chemistry were reported.[55−58] Their synthetic strategy is similar

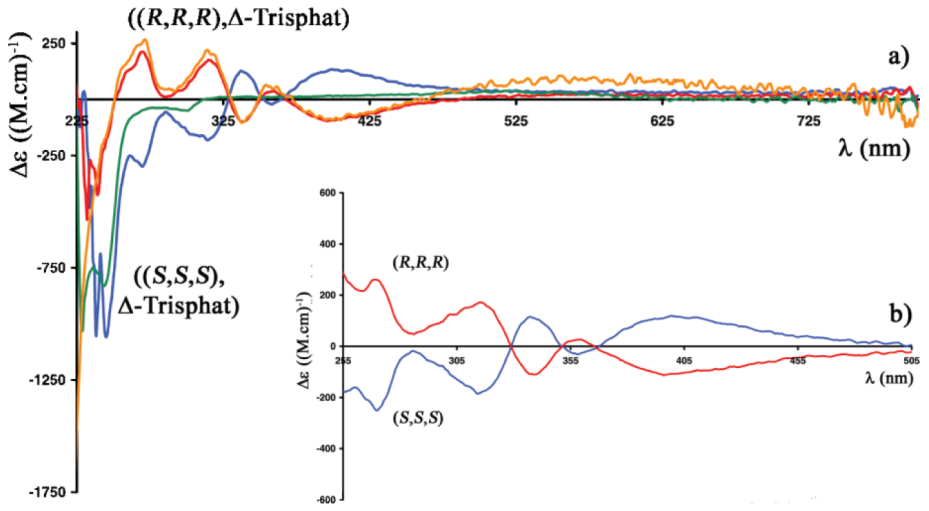

Figure 3. (a) CD traces for the X-ray analyzed crystal **8a** ((*R,R,R*), Δ-TRISPHAT) (orange line), sample 2 enriched **8a** ((*R,R,R*), Δ-TRISPHAT) (red line), sample 1 enriched **8b** ((*S,S,S*), Δ-TRISPHAT) (blue line), and [*n*-Bu_4N][Δ-TRISPHAT] (green line) recorded in CH_2Cl_2 solution and at the same concentration (0.03 mM). (b) CD curves of only the two enantiomers (*R,R,R*) and (*S,S,S*) after subtraction of the curve due to the Δ-TRISPHAT anion.

Scheme 6. Synthesis of Ruthenium Metallaprism and Inclusion of Aromatic Guests

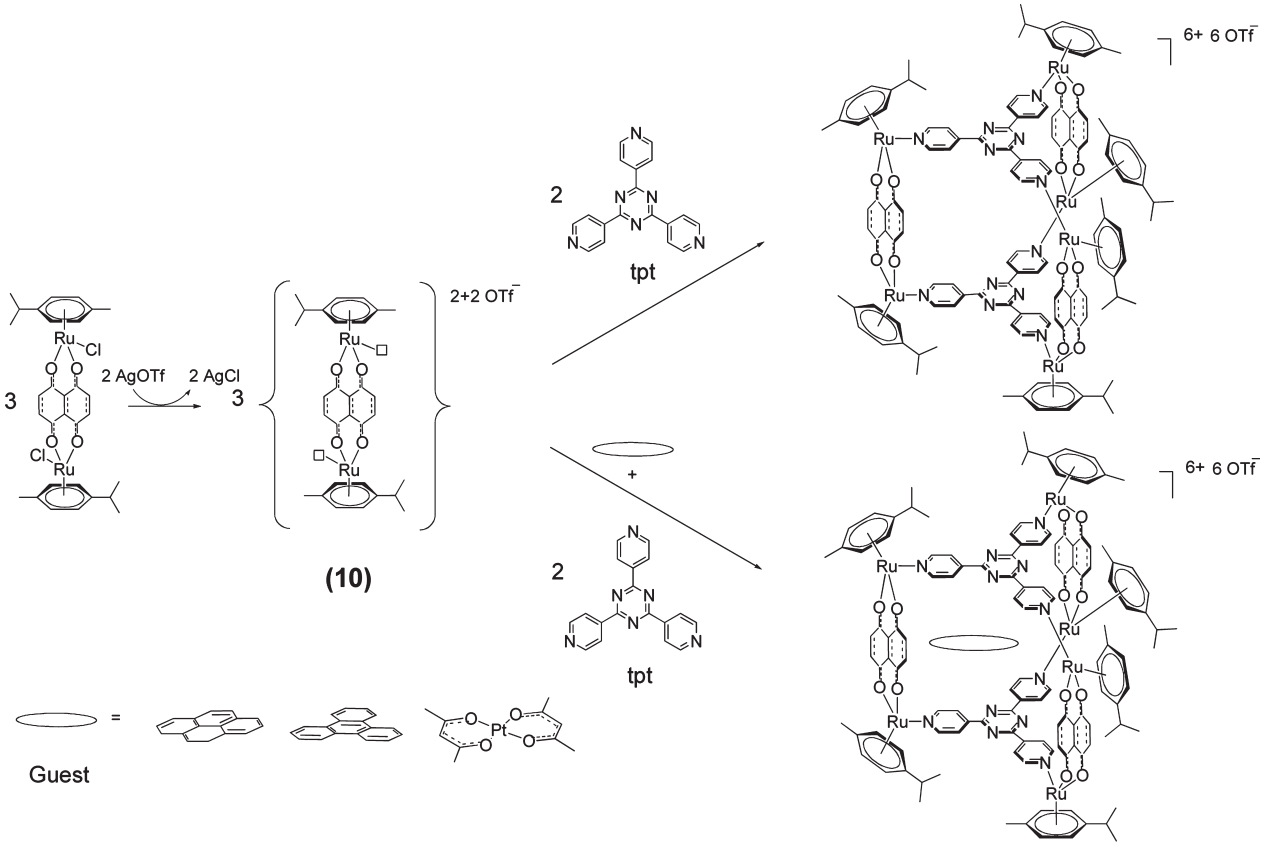

to that described in the previous section; the first step involves the preparation of linear binuclear connectors from [(arene)M(μ-Cl)Cl]$_2$ and a rigid tetradentate ligand such as 1,4-dihydroxyanthraquinone (H2OX), 1,4-dihydroxybenzoquinone (H2DHBQ), 2,5-dichloro-3,6-dihydroxy-1,4-benzoquinone (H2CA), 6,11-dihydroxy-5,12-naphthacenedione (H2DHNQ), etc. in the presence of a base. Subsequent treatment with bifunctional pyridyl ligands in the presence of AgOTf provides the target tetranuclear molecular rectangles. Interestingly when an olefin unit is present in the bifunctional pyridyl linker 4,4′-bpe (bpe = *trans*-1,2-bis(4-pyridyl)ethylene), the tetranuclear metalated rectangles (**12** and **13**) were active toward [2 + 2]-photocycloaddition

dx.doi.org/10.1021/cr200345v |*Chem. Rev.* 2012, 112, 2015–2041

mediated by UV−visible as light source.[59] This photodimerization occurs in the solid state on single-crystal-to-single-crystal transformation mediated by the Cp*Ir molecular bricks in the linear templates (Scheme 7).

Réau and co-workers reported the synthesis of a unique class of metallorectangles by taking advantage of a U-shaped molecular clip designed by the authors.[60−63] The latter is based on copper dimers bridged by two phosphole ligands as well as phosphole and dppm ($Ph_2PCH_2PPh_2$) (Scheme 8). These molecular clips react with cyano-capped π-conjugated linkers to give a family of π-stacked metallocyclophanes (**14**). In these metallorectangles the π-walls of the conjugate linkers have an almost face-to-face arrangement with $\pi-\pi$ contacts of 3.4−3.5 Å. Remarkably metallocyclophanes with nanoscopic sizes were obtained with an intermetallic distance up to 31.5 Å. The authors consider the supramolecular assembly as the longest metallorectangle ever reported.[64]

2.5. Metallomacrocycles and Anion Encapsulation

Metallomacrocycles based on piano-stool $Cp^*ML^1L^2L^3$ bricks were also employed to study the encapsulation of counteranions; however, there are only a few examples reported in the literature.[24] Thus, Kojima, Fukuzumi, and co-workers described the preparation of a tetranuclear iridium coordination assembly bridged by a flavin-type ligand. This supramolecular species **15** possesses a U-shaped structure as confirmed by single-crystal X-ray diffraction study (Scheme 9). The structure also shows that a PF_6 anion is included in the U-shaped cavity, and the species occurs as a dimer of tetranuclear species associated via hydrogen bonding.

Scheme 7. Tetranuclear Metallorectangles 12 and 13 Showing [2 + 2]-Photocycloaddition

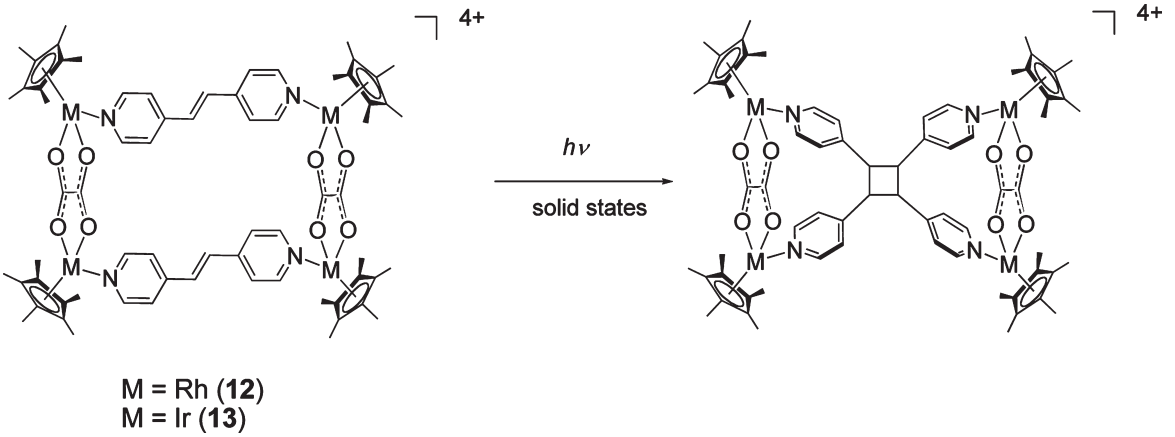

Scheme 8. Metallorectangles with π-Conjugated Linkers

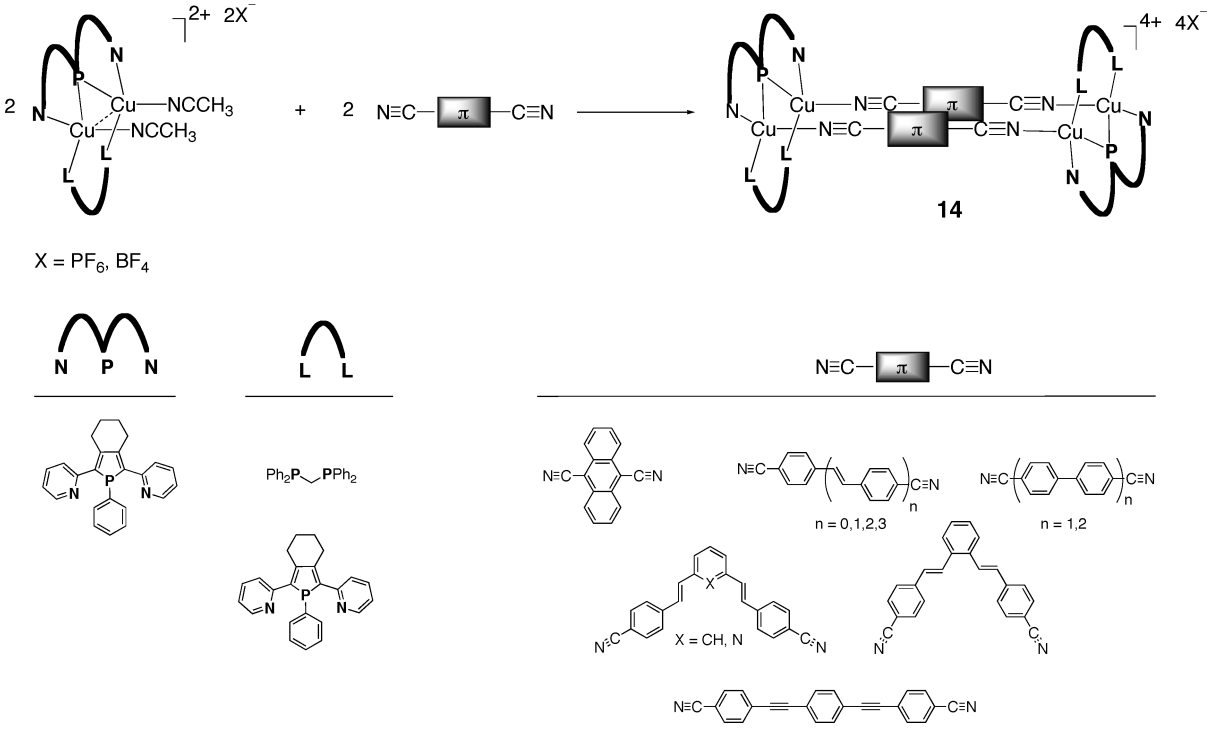

dx.doi.org/10.1021/cr200345v |Chem. Rev. 2012, 112, 2015–2041

Scheme 9. Tetranuclear Iridium 15 Assembly with U-shaped Cavity Showing Anion Exchange of PF_6 by ClO_4

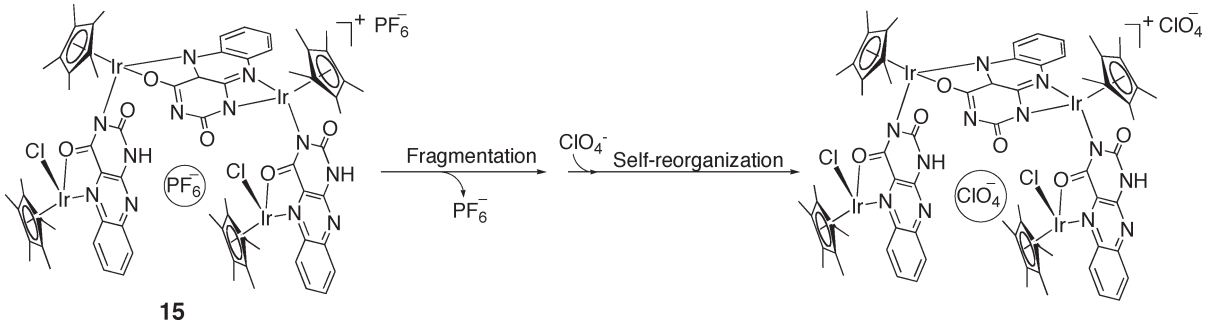

15

Further solution studies show that the host system undergoes an anion exchange with replacement of the guest counteranion PF_6 with ClO_4.[65]

More recently, Jin and co-workers reported the self-assembly of metallocycles incorporating 4−6 half-sandwich (arene)M {arene = Cp*, *p*-cymene} as metal corners linked by pyridyl-substituted diketone bridging ligands. The X-ray molecular structure showed that these large hexanuclear coordination assemblies could be described as trigonal antiprisms. The structure also shows that one of the counteranions, whether PF_6 or OTf, is encapsulated inside the cavity of the host assembly. Weak hydrogen bonding between guest anions and C(sp^3)−H of the methyl group pointing toward the inside of the cavity and electrostatic interactions between host and guest are at the origin of such encapsulation.[56]

Indeed such types of interactions were also observed by Amouri and co-workers in a rare example of supramolecular assembly [Cp*Ir(η^6-$C_6H_2O_4$)$(BF_2)_2(CF_3SO_3)$][Cp*Ir(μ-Cl)$_3$-IrCp*] (**16**). Remarkably, the X-ray molecular structure of **16** shows that an anion−π interaction occurs between the neutral component Cp*Ir(η^6-$C_6H_2O_4$)$(BF_2)_2$ of the assembly and the CF_3SO_3 counteranion of the cationic species [Cp*Ir(μ-Cl)$_3$-IrCp*] (Figure 4).[66] Computational studies show that this non-covalent interaction can be better described as a combination of hydrogen bonding between the C(sp^3)−H methyl groups of the Cp*Ir moiety and the oxygen centers of the triflate anion and also due to anion−π interaction manifested through short C···O contacts of 2.940 Å for C4−O3 and 3.196 Å for the two C6−O4 interactions, which are symmetrically related via the molecule plane of symmetry. These bond distances are shorter than the sum of their van der Waals radii (d = 3.22 Å).[67] These results illustrates the power of Cp*M to act itself as an anion acceptor,[68] which thus may impede the encapsulation of a guest anion inside the confined spaces available in such host assemblies based on Cp*M as metal corners. This result explains why host−systems based on Cp*M bricks that act as anion receptors remain rare.

The next section describes the self-assembly of metallocages based on a variety of metal bricks that lack a Cp*M unit and form nanocavities available to encapsulate weakly coordinating anions.

3. COORDINATION NANOCAGES TEMPLATED BY WEAKLY COORDINATED ANIONS

3.1. Generalities

Anion-template approaches continue to be an important subject in supramolecular coordination chemistry.[4,69−72] These studies made possible the emergence of metal-based anion receptors.[5,73] The presence of a metal center in a coordination assembly may play a crucial role in anion recognition due to its intrinsic property to bind anions and also to organize the formation of the final assembly. Such coordination assemblies have shown a wide range of applications in biochemistry, environment, recognition, ion exchange, and chemical sensors.[74−76] Several reviews have appeared recently describing coordination chemistry of anions or anion templation strategy to form a variety of assemblies with different size and topology.[77−84] Previous reviews cover a variety of metallomacrocycles that do not possess a well-defined cavity or confined space for anion encapsulation. Therefore, such examples will not be discussed in this review; however, our attention will be devoted to discrete three-dimensional metallo-assemblies that possess a confined space for hosting anions inside their cavity.

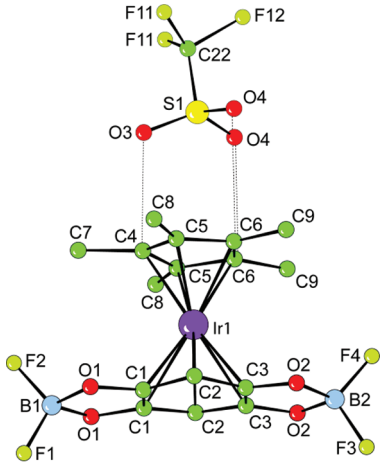

Figure 4. (a) View of the anionic part of the assembly [Cp*Ir(η^6-$C_6H_2O_4$)$(BF_2)_2(CF_3SO_3)$]$^{-1}$ with atom numbering system. (b) The CF_3SO_3 anion is perfectly located on top of Cp*Ir and lies on the same plane of symmetry as that of [Cp*Ir(η^6-$C_6H_2O_4$)$(BF_2)_2$]. (c) C···O short contacts are shown by dotted lines.

3.2. M_2L_2 and Related Accommodating Weakly Anion Guests

Metallocages of the type M_2L_2 (M = metal, L = ligand), M_2L_3, M_2L_4, M_3L_2, or M_4L_6 were obtained by self−assembly. Some of these showed properties as hosts to anions. In fact their formation is often directed by the anion guest, which acts as a template. For instance, metallacages of the type Ag_2L_2 and Ag_2L_3 were

dx.doi.org/10.1021/cr200345v |*Chem. Rev.* 2012, 112, 2015–2041

Scheme 10. Schematic Representation of the Preparation of the M_2L_4 Boxlike Complex $\{[PF_6\subset Pd_2(L^1)_4][PF_6]_3\}$ (17)

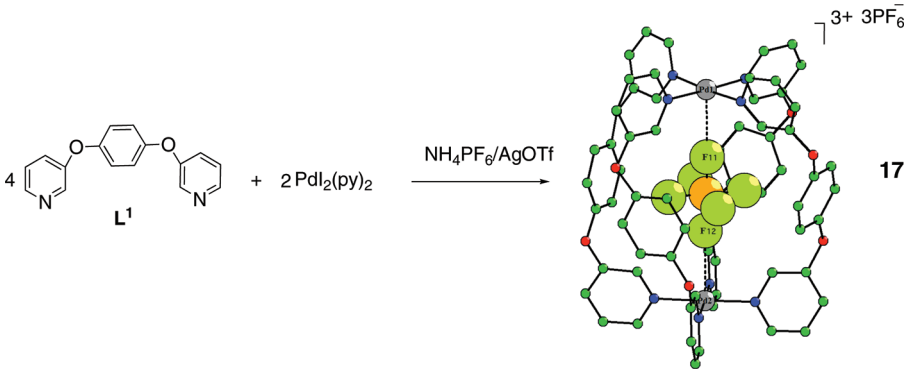

prepared from flexible linear or tripodal exodentate ligand such as 1,4-bis(benzimidazol-1-ylmethyl)2,4,6-trimethylbenzene or 1,3,5-tris(imidazol-1-ylmethyl)benzene and silver salts AgX (X = SbF_6^- > PF_6^- > BF_4^- > ClO_4^-). These metallo-hosts contain a weakly coordinating anion inside their cavity.[85−90] Furthermore, a zwitterionic dicopper helicate was also reported, in which an anion of the type X = SO_4^{2-}, ClO_4^-, HPO_4^{2-}, NO_3^-, BF_4^-, or I^- could be encapsulated.[91] The authors demonstrated in solution that the helicate is capable of binding anions in a 1:1 ratio of helicate to anion, in the order SO_4^{2-} > HPO_4^{2-} > ClO_4^- ≈ NO_3^- ≈ BF_4^-.

Among the most appealing metallocages are of the type M_2L_4. In this context a saturated quadruply stranded helicate of formula $\{[PF_6\subset Pd_2(L^1)_4][PF_6]_3\}$ (**17**) exhibits selective encapsulation of a PF_6^- anion inside the cavity.[92] The synthesis of **17** can be realized in a direct manner by self-assembly between $[PdI_2(py)_2]$ (py = pyridine) and 1,4-bis(3-pyridyloxy)benzene ligand L^1 in a ratio 1:2 in the presence of AgOTf and NH_4PF_6 (Scheme 10).

The molecular structure of **17** revealed the formation of a $Pd_2(L^1)_4$ box and a PF_6^- anion located inside the cavity through a metal−anion coordination bond. Weak contacts between the two Pd centers and the encapsulated PF_6^- were observed with Pd1----F11 of 2.789(5) Å and Pd2----F12 of 2.911(5) Å. The three other anions are located outside the cavity. The integrity of the metallocage has been shown to be maintained in solution by NMR and fast atom bombardment (FAB) spectroscopy. Remarkably, the ^{19}F NMR spectrum appeared as two sets of doublets attributed to the encapsulated and free anion. The authors suggest that in solution the encapsulated PF_6^- anion remains inside the cage but is tumbling within the confined space of the cavity.

3.3. M_2L_4 Nanocapsules and Unusually Weakly Encapsulated Anions

In 2005, our group reported the first coordinated unsaturated cobalt-based M_2L_4 boxes and demonstrated their properties as hosts for tetrafluoroborate anion.[93] Our strategy was completely different to that of the metallohelicate described previously based on the use of a cobalt salt precursor $Co(II)(BF_4)_2.6H_2O$ and 1,3-(bis(benzimidazol-1-ylmethyl)-2,5-dimethoxy-4,6-dimethylbenzene L^2 as assembling connector to provide a coordinatively unsaturated cobalt center with weak interaction to the guest anion. A family of highly symmetrical unsaturated tetragonal cobalt cages $\{[BF_4\subset(MeOH)_2Co_2(L^2)_4][BF_4]_3\}$ (**18**) and $\{[BF_4\subset(R\text{-}CN)_2Co_2(L^2)_4][BF_4]_3\}$ (**19**−**21**) (R = CH_3, Et, Ph) were prepared. (Scheme 11)

Scheme 11. Schematic Representation of the Preparation of the M_2L_4 Boxlike Assembly $\{[BF_4\subset(MeOH)_2Co_2(L^2)_4][BF_4]_3\}$ (18) and $\{[BF_4\subset(R\text{-}CN)_2Co_2(L^2)_4][BF_4]_3\}$ (19−21) (R = CH_3, Et, Ph)

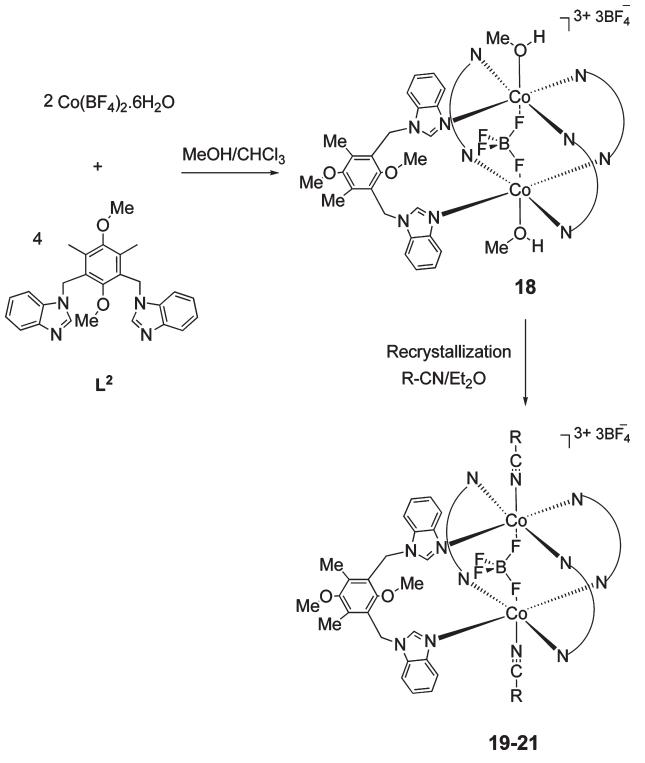

A single X-ray structure determination of $\{[BF_4\subset(CH_3\text{-}CN)_2Co_2(L^2)_4][BF_4]_3\}$ (**19**) was carried out to determine the identity of this compound and revealed the formation of a M_2L_4 tetragonal cage. In this metallocapsule each square-pyramidal cobalt atom is coordinated to four nitrogen atoms from four bridging ligands (in the equatorial position). Furthermore, the cobalt center is coordinated to a solvent molecule (in the apical position). The structure shows a unique BF_4^- anion located in the middle of the confined cavity (Figure 5). The unsaturated cobalt ion binds also to a fluorine atom from a BF_4^- anion through a metal−anion interaction with Co----F 2.405 Å. Additionally, external to the cage are located the other three BF_4 anions. The dimension of the box is defined by the Co−Co

dx.doi.org/10.1021/cr200345v |*Chem. Rev.* 2012, 112, 2015–2041

[Co1−Co1] separation of 7.1 Å, and the distance between two facial benzene rings is 11 Å.

The NMR and FAB mass spectrum studies ascertained the integrity of this assembly in solution. Indeed, the ^{1}H NMR spectrum of $\{[BF_4 \subset (CH_3CN)_2Co_2(\mathbf{L^2})_4][BF_4]_3\}$ (**19**) was recorded, and the spectrum observed spanned a broad range, consistent with the presence of a Co(II) paramagnetic center. All the signals were then assigned based on the analysis of T_1 relaxation times for the individuals signals, which correlates with the sum of the r^{-6} distances from each of the Co(II) atoms. To our knowledge, this was the first example described in the literature in which all the signals of a paramagnetic Co(II) assembly were assigned. Moreover, the ^{11}B NMR spectrum of this cage showed not only the presence of a singlet around 1 ppm attributed to free anions but also a broad signal at −105 ppm corresponding to the encapsulated BF_4^- anion. Variable-temperature (VT) NMR studies showed that no exchange between the encapsulated anion and the free BF_4^- was possible. Although the tetrafluoroborate anion is sequestered in the metallocage, we feel it may be spinning or tumbling within the cavity rather than being locked in one defined position.

To determine the role of the BF_4^- in the self-assembly process of the above metallocages, experiments were carried out using other coordinating anions. Indeed, switching to $CF_3SO_3^-$, NO_3^-, and Cl^- allowed the formation of different supramolecular architectures; however, no metallocages were obtained.[94] These results illustrate the effect of the BF_4^- as a templating anion. In a similar manner, a relevant example of anion, which acts as template to determine the nature of the final isolated structure, was described in 2005 by Dunbar and co-workers in which the self-assembly process between the divergent bispyridine bidentate organic spacer 3,6-bis(2-pyridyl)-1,2,4,5-tetrazine (bptz) and solvated transition metal ions M(II) (M = Ni, Zn) can be controlled by the nature of the counteranion.[95]

Hexafluorophosphate and tetrafluoroborate are weakly coordinating anions and often show similar behavior in the self-assembly of nanocages and coordinaton polymers.[96,97] However, the latter is smaller in size and possesses a tetrahedral geometry. Thus, efforts to construct analogous Co_2L_4 nanocages with weakly coordinating anions such as PF_6^- anion were realized.[98] Using a similar procedure but mixing $[Co(CH_3CN)_4][PF_6]_2$ with ligand $\mathbf{L^2}$ in acetonitrile gave the expected dinuclear tetragonal capsule $\{[PF_6 \subset (CH_3CN)_2Co_2(\mathbf{L^2})_4][PF_6]_3\}$ (**22**) (Figure 6).[98]

The crystallographically determined structure of **22** shows a comparable M_2L_4 tetracationic box in which the cobalt centers bind also to an anion located inside the cavity via a metal anion coordination: [Co-----F] 2.361 Å, [Co----F] 2.426 Å. The other three anions are located outside, two of which interconnect two capsules via C−H---F interactions to form a 1D supramolecular chain of 3D nanocapsules.

Solution ^{1}H NMR analysis confirmed that the integrity of **22** is maintained in solution. Moreover, the solid-state ^{31}P and ^{19}F NMR investigations were used to confirm the location of the PF_6 anion inside the cavity.

These results suggest that both BF_4^- and PF_6^- guests are suitably designed for our Co_2L_4 hosts. Further anion competitive investigations demonstrated that Co_2L_4 nanocages are selective toward BF_4^- over PF_6^- anions. At this point, a comment on the behavior of such Co_2L_4 hosts is noteworthy. In fact, although the octahedral geometry of the PF_6^- anion may show a better fit relative to the solid-state structure of the cobalt host, we note that the anion size favors the BF_4^- and is therefore more adequate

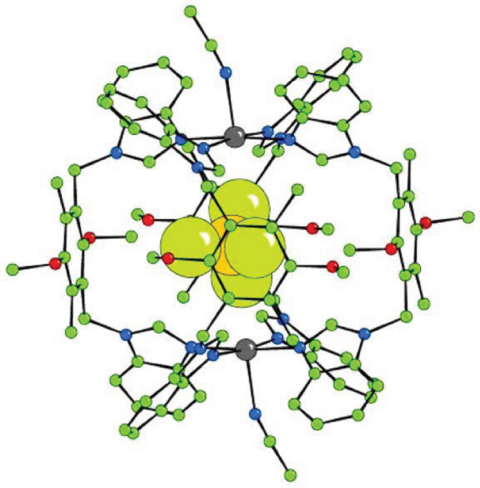

Figure 5. Molecular structure of $[BF_4 \subset (CH_3CN)_2Co_2(\mathbf{L^2})_4]^{3+}$ showing the encapsulated BF_4 anion.

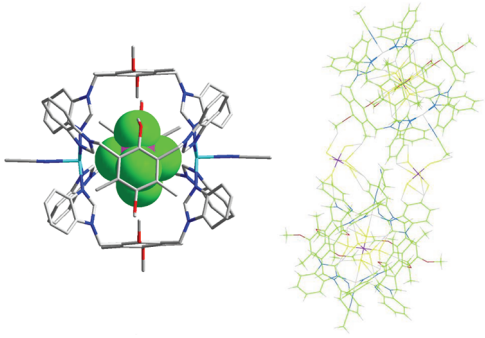

Figure 6. (a) Molecular structure of $\{[PF_6 \subset (CH_3CN)_2Co_2(\mathbf{L^2})_4]^{3+}$ showing the encapsulated PF_6^- anion. (b) 1D chain of 3D capsules formed via weak hydrogen bonding between individual molecules via two external PF_6^- anions.

within the confined space. All in all, we feel that our Co_2L_4 cages represent an interesting class of nanocages with selective recognition to weakly BF_4^- anion. In fact, the role of this anion is also highlighted in the next paragraph where a rare example of a Co_2L_4 cage templated by three weakly coordinating anions could be isolated.

Thus, the preparation and characterization of a novel cobalt capsule, in the absence of coordinating solvent, was reported.[84] Using a similar experimental procedure but in nitromethane instead of CH_3CN or MeOH provided a new host−guest cage $\{[BF_4 \subset (BF_4)_2Co_2(\mathbf{L^2})_4][BF_4]\}$ (**23**) quantitatively. An X-ray structural determination of **23** revealed the formation of a novel type of tetragonal M_2L_4 cage in which there are two externally coordinated BF_4 anions that bind directly to the cobalt center (in the apical position) instead of solvent molecules with [Co----F] = 2.187 Å. Moreover, a third BF_4^- anion is located inside the cavity of the cage, and a weak metal anion interaction with [Co----F] = 2.312 Å was observed. Compared to previous capsules this distance is slightly smaller, leading to a slightly smaller cavity size of 6.9 Å × 10.7 Å × 10.7 Å (Figure 7).

As previously, ^{1}H and ^{11}B NMR spectra are in agreement with the proposed formula of **23**. Moreover, solution electrospray mass spectroscopy confirmed that the capsule remains intact in

solution. To the best of our knowledge, this is a rare example of a cage that exhibits coordination of three fluorinated weakly binding anions, one sequestered inside the cavity and the two others externally bonded to the cobalt centers. Zhang, Hong, and co-workers have, however, reported some Co_2L_4 capsules (L = 1,3-bis-(pyrid-4-ylthio)propan-2-one) in which three coordinating halides anions (Br^- or Cl^-) are directly bonded to two cobalt(II) centers.[99] However, in this example strongly coordinated anions were used.

We then extended our methodology to tetragonal Cu(II) capsules, which are rare. Atwood and co-workers described a tetragonal dicopper nanocapsule in which the four equatorial positions of each Cu(II) atom are occupied by four pyridyl groups of exobidentate ligands.[100] The axial positions are occupied by water molecules, and four nitrate anions are located inside the nanocage. Dinuclear copper complexes of the M_2L_4 family including a perchlorate anion between the two metal centers were also reported.[85]

Following our experimental approach, two tetragonal copper(II) cages $\{[BF_4\subset(CH_3CN)_2Cu_2(\mathbf{L^2})_4][BF_4]_3\}$ (**24**) and $\{[BF_4\subset(BF_4)_2Cu_2(\mathbf{L^2})_4][BF_4]\}$ (**25**) were prepared (Scheme 12).[101]

The structure of **25** shows the formation of a novel type of Cu_2L_4 tetragonal cage that encapsulates a BF_4^- anion inside the cavity with a Cu---F weak interaction of 2.461 Å. (Figure 8) Moreover, two coordinated anions bind externally (apical positions) to the two copper centers with Cu----F 2.475 Å. This compound constitutes another example of metallocages where three BF_4^- anions are coordinated to the copper centers.

Wang and co-workers described more recently the use of a ditopic ligand $\mathbf{L^3}$ [1,3-bi(imidazol-1-ylmethyl)-2,4,6-trimethylbenzene] with copper(II) nitrate hexahydrate in a methanol−acetonitrile solution to lead to the metallocage $\{[(NO_3)(MeOH)\subset Cu_2(NO_3)_2(\mathbf{L^3})_4][NO_3]\}$ (**26**).[102] The X-ray diffraction analysis confirmed the formation of this M_2L_4 metallacage and revealed the presence of a nitrate and a methanol molecule inside the cavity. On the other hand, Kim and co-workers described the preparation of an inorganic tennis ball compound $\{[BF_4\subset Cu_2(\mathbf{L^4})_4][BF_4]_3\}$ (**27**) (Scheme 13) where $\mathbf{L^4}$ = (dach)Pt^{II}(BETMP) (dach = *trans*-1,2-diaminocyclohexane and BETMP = bisethylthiomethylidenepropanedioate). In solution the Cu−Pt assembly dimerizes and encapsulates a BF_4 anion to give **27**.[103] The term tennis ball was coined by Rebek and co-workers and describes the formation of a spherical dimer of the glycouril derivative prepared by condensing two molecules of diphenylglycouril with durene tetrabromide.[104]

In copper cage **27** the authors suggest that the anion interacts with the two copper atoms and should constitute an essential driving force during the self-assembly process. A related compound with ClO_4^- anion inside the cavity of the tennis ball was prepared. The authors have also found that the tennis ball compounds showed different selectivity toward the anions; for instance, ClO_4^- is preferentially encapsulated rather than BF_4^-.

In summary, this section described the preparation of three-dimensional M_2L_4 metallocages templated by weakly coordinating anions. In some of these capsules, the weakly coordinated anion undergoes an unusual interaction with the metal centers. In the next paragraph we describe the construction of other capsules of type M_4L_6 possessing larger cavities capable of encapsulating not only weakly coordinating anions but also a variety of molecular guests.

3.4. M_4L_6 Nanocapsules Accommodating Weakly Anion Guests

Tetrahedral cages of type M_4L_6 are generally obtained by self-assembly between a metal ion with preferably an octahedral geometry and a bisbidentate ligand in a ratio 4M/6 L. These hosts are suited to encapsulate anions and molecules as well.

Heinze and co-workers reported the synthesis of the tetrahedral host−guest complexes from six bidentate ligands fumaronitrile and its saturated derivative succinonitrile $\mathbf{L_n^5}$ = $N{\equiv}C{-}C_2H_{2+n}{-}C{\equiv}N$ (C_2H_{2+n} = C_2H_2 for n = 0 and C_2H_4 for n = 2) and four Fe(II) metal centers capped with triphos

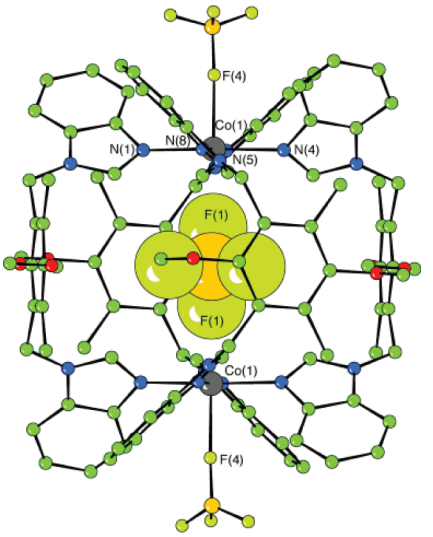

Figure 7. Molecular structure of the cationic part of **23** showing one encapsulated and two other coordinated BF_4 anions.

Scheme 12. M_2L_4 Boxlike Assemblies $\{[BF_4\subset(CH_3CN)_2Cu_2(\mathbf{L^2})_4][BF_4]_3\}$ (24) and $\{[BF_4\subset(BF_4)_2Cu_2(\mathbf{L^2})_4][BF_4]\}$ (25)

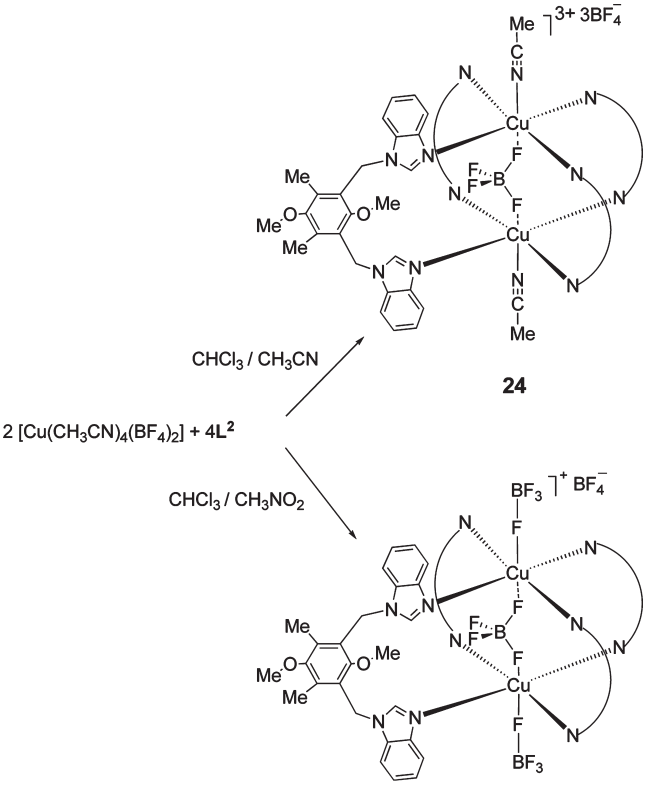

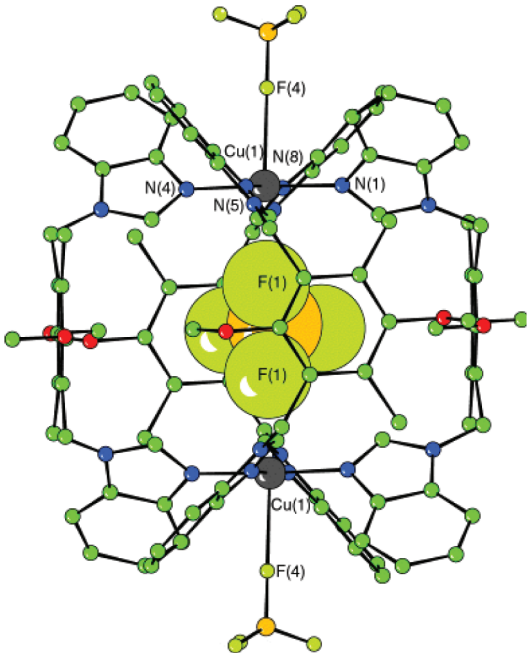

Figure 8. Molecular structure of the cationic part of **25**.

Scheme 13. Schematic Representation of the Tennis Ball Assembly $\{[BF_4{\subset}Cu_2(L^4)_4][BF_4]_3\}$ (27)

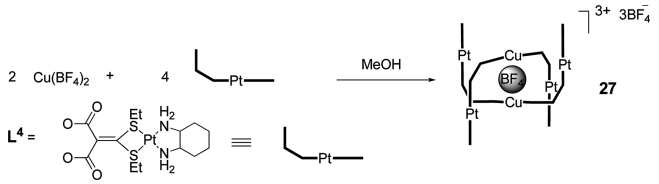

ligands to give the tetrahedra cages $\{[BF_4{\subset}(triphosFe)_4(L_n^5)_6][BF_4]_7\}$ (**28** and **29**) (Scheme 14).[105]

The authors suggest that the formation of the self-assembled tetrahedron complex is perhaps driven by the symmetry match between the tetrahedron host and the anionic guest.

Lindoy and co-workers reported the preparation and characterization of new tetrahedral capsules of the type $Fe_4L^6{}_6$ (**30**) capable of encapsulating fluorinated anions PF_6^- and BF_4^- in their cavities.[106] In general these assemblies are maintained by a rigid linear bisbidentate quaterpyridine ligand $\mathbf{L^6}$ and show selectivity for PF_6^- over BF_4^-. Each metal vertex is chiral and adopts either a Δ or Λ configuration. Very recently the same group described the inclusion of $[FeCl_4]^-$ anion with such a tetrahedral cage.[107]

Ward and co-workers have used a series of bidentate flexible ligands $\mathbf{L^7}$ based on two pyrazolyl−pyridine binding sites separated by an *o*-xylyl spacer to prepare a variety of tetrahedral cages from divalent metal centers that are capable to host anions of different shapes. Once again, such metallocages are chiral. In fact, the four metal centers are tris-chelated, and thus, each metal possesses either a Δ or Λ configuration. The assembled capsule $\{[BF_4{\subset}Co_4(L^7)_6][BF_4]_7\}$ (**31**) was obtained quantitatively and encapsulates one BF_4^- anion (Figure 9).[108]

In this host−guest system, the common tetrahedral geometry represents a driving force for the encapsulation process. The X-ray structural determination of this cage revealed that each fluoride center of the encapsulated anion is directed to the center of a Co_3 triangular face (Figure 9). Further, there are some C−H---F contacts due to interactions between the fluorine atom and the CH_2 spacer of the bispyrazolyl−pyridine ligand $\mathbf{L^7}$.

In solution, VT NMR ^{11}B and ^{19}F NMR studies revealed that this anion is trapped inside the cavity and no exchange with the free anions was observed. However, the authors showed that, when the bridging ligand is bigger, the cavity size becomes larger, leading to higher rates of ion exchange.

Ward and co-workers described also the formation of tetrahedral Co(II) and Zn(II) cages of general formulas $\{[X{\subset}M_4(L^8)_6][X]_7\}$ using modulable bisbidentate ligand $\mathbf{L^8}$ [109,110] (Table 1, entries a, b, d, g, and h). In these cases the encapsulated anion appeared to be a perfect fit in terms of size and shape. Indeed, the O or F atom of the encapsulated anion interacts with the CH_2 groups of the ligands via, respectively, CH---O and CH---F hydrogen bonds, and the tetrahedral anion is completely encapsulated so that no exchange was observed with free anions. This result implies that the anion guest acts as a template around which the cage self-assembles. More recently the preparation of cages based on Cd(II) (Table 1, entry f) and encapsulating one hexafluorosilicate (Table 1, entry e) anion were also reported.[111] The use of chiral bispyrazolyl pyridine ligand (Table 1, entries c and j) to form the expected tetrahedral cages $\{[X{\subset}Zn_4(L^8)_6][X]_7\}$ ($X = BF_4^-$, ClO_4^-) was described.[112,113] A diastereoselective formation of the preferred isomer was observed. Such metallocages crystallized in a chiral space group, and a single enantiomer was formed. The chirality of the pinene present on the assembling ligand dictated the sense of the chirality of the four-homochiral metal centers at the corners. Interestingly, the configurations of these metal centers were dependent on the ligand spacer rather than the absolute configuration of the pinene group itself. For instance, these configurations are opposite with 2,3-naphthalene as ligand spacer instead of 1,2-phenylene. The formation of larger tetrahedral cages by using ligand including a biphenyl group as spacer (Table 1, entry i) and Co(II) salts was also reported.[114] Tetrahedral capsules possess larger cavities that accommodate a wide range of different anions. As a consequence, exchanges between encapsulated and free anions were observed at room temperature in the ^{19}F spectra. Additionally, by modifying slightly the topology of the bisbidentate pyrazolyl−pyridine ligand, unexpected M_8L_{12}, $M_{12}L_{18}$, and $M_{16}L_{24}$ cages possessing larger cavities were obtained.[5,115−117] Contrary to the smaller M_4L_6 metallocages, the larger assemblies possess an open structure and may contain more than one anion inside their cavities, implying that the guests are not really encapsulated. To counterbalance this effect, incorporation of functionalities into ligands may be an alternative strategy for the anion sequestration.

Indeed, another approach for the construction of a M_4L_6 tetrahedral cage has been reported by Custelcean, Hay, and coworkers. The authors used the *HostDesigner* software to construct a sulfate-encapsulating receptor. Thus, the metallocage $\{[SO_4{\subset}Ni_4(L^9)_6][SO_4]_3\}$ (**32**) was assembled in a water−methanol media using $\mathbf{L^9}$, a bisbipyridine urea ligand containing simple $-CH_2-$ linkage.[118] In this system, 12 hydrogen-bonding sites were positioned in the cavity and placed to complement the geometric and polar requirements of sulfate anion to form a $[SO_4(\mathbf{urea})_6]^{2-}$ complex structure (Figure 10).

In this section, we described the preparation of tetrahedral metallocages possessing host−guest properties with weakly coordinating anions. M_4L_6 capsules are not limited, however,

Scheme 14. Preparation of the M_4L_6[5] Tetrahedra Complexes $\{[BF_4\subset(triphosFe)_4(L_n^5)_6][BF_4]_7\}$ ($n = 0, 28$; $n = 2, 29$); Molecular Structure of Complex 28

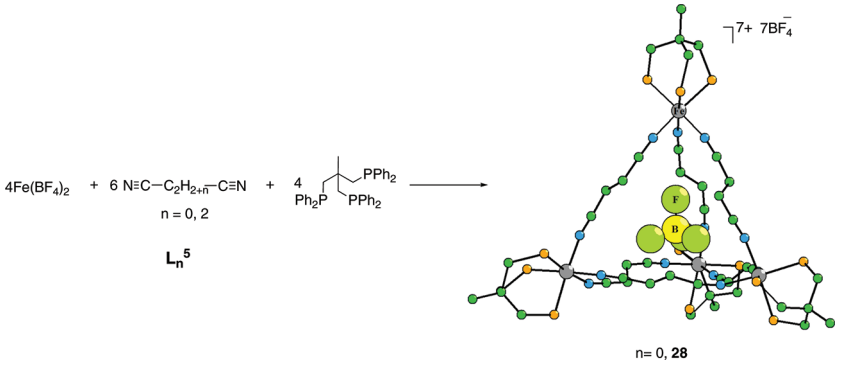

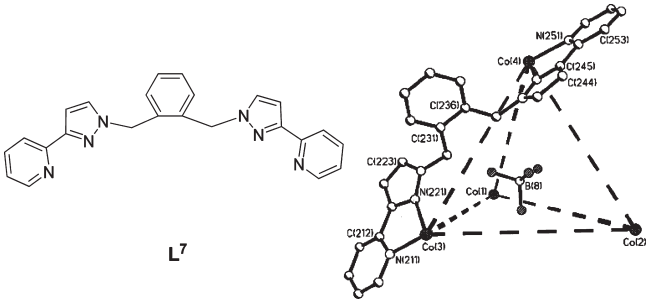

Figure 9. Ligand L^7 and the structure of the related assembly with one encapsulated BF_4 anion.

to the encapsulation of such species. Examples in which the hydrophobic central cavity of metallocage accommodates organic compounds and hazardous substances as well have appeared in the literature. For example, Nitschke and co-workers reported recently the preparation of a self-assembled M_4L_6 capsule $\{[P_4\subset Fe_4(\mathbf{L^{10}})_6]^{4-}\}$ (**33**) capable of sequestration in its cavity a pyrophoric white phosphorus P_4.[119] Remarkably, this substance becomes air-stable and water-soluble within the hydrophobic hollows of the self-assembled tetrahedral container molecules (Figure 11).

The authors attributed this remarkable stability to the constriction applied by the confining capsule, with the reaction between O_2 and P_4 generating an intermediate compound too large to be encapsulated in the cavity. This example illustrates how the reactivity of a compound can be affected in the confined-space environment of a metallocage.

Very recently Nitschke and co-workers extended their approach to prepare higher coordination capsules of $Fe_8(M{-}\mathbf{L^{11}})_6$ stoichiometry (Scheme 15). This chiral cubic cage was obtained by mixing six tetrakis-bidendate porphyrin-based ligands $M{-}\mathbf{L^{11}}$ formed in situ ($M{-}\mathbf{L^{11}}$ = $H_2{-}\mathbf{L^{11}}$, $Ni{-}\mathbf{L^{11}}$, $Zn{-}\mathbf{L^{11}}$) and 8 equiv of $Fe(OTf)_2$. The porphyrin-faced $[Fe_8(M{-}\mathbf{L^{11}})_6]$-$[OTf]_{16}$ hollow cubic assemblies displayed large cavities (>1300 Å^3) capable of encapsulating large aromatic guests.[120] Indeed, 3 equiv of coronene molecules were hosted inside the cavity through $\pi{-}\pi$ interactions. Interestingly, this M_8L_6 nanocapsule showed selectivity toward encapsulating higher fullerenes from fullerene soot.

It is, therefore, of interest to envisage the use of these metallocapsules as nanoreactors for chemical transformation. Relevant examples of such capsules will be discussed later.

4. NANOCAGES FOR MOLECULAR ACTIVATION AND TRANSFORMATION

4.1. Nanocages Based On "PdL_2" Building Blocks As Molecular Flasks

The use of metal containing building blocks that can direct the self-assembly to form endohedral macrocycles and nanocapsules with large cavities has been the focus of intensive research in supramolecular coordination chemistry.[121−124] In this context Fujita and co-workers reported the preparation of self-assembled coordination cages **34** and the nanobowl **35**.[125−128] The judicious choice of a square-planar building block $(N^{\wedge}N)Pd^{2+}$ with bidentate ethylenediamine ligands is to enforce a 90° cis coordination geometry around the metal ion. Thus treatment of square-planar metal ions with tridentate trispyridyltriazine paneling ligand led to the formation of either an octahedral cage **34** or a square-pyramidal bowl-shaped structure **35** (Figure 12). These structures are highly charged (+12), and the use of nitrates as counterions confers to these species high water solubility. The four triazine panels occupy alternate faces of the octahedron **34** whereas the pyramidal bowl-shaped complex **35** possesses one open face, providing in both cases a large hydrophobic cavity. These well-defined cavities are capable to accommodate a variety of hydrophobic organic guest molecules. The size and the shape of the cavity are important parameters, which alter the reactivity and properties of encapsulated substrates.

In fact, guest encapsulation may lead to the formation of unexpected intermolecular interactions, which give rise to new physical properties. For example, alteration of redox properties of ferrocenes or unconventional intramolecular interaction of nitroso organic radicals was reported by Fujita and co-workers using **34** as a molecular flask.[129−132] Moreover, considering their nanosized space in which reactive compounds can be protected and stabilized, assemblies **34** and **35** can be employed as containers.[133] Thus, reactive species are generated in situ and trapped. The latter arises from mixing of starting materials in the nanovessel coordination assembly. For instance, molecular flasks **34** and **35** are capable of accommodating, respectively, two and three stable trialkoxysilanes. Their polycondensation generates, respectively, kinetic short-lived silanol trimers and dimers that remain stable within the cages despite the presence of their highly reactive SiOH groups, which under normal conditions should favor the formation of tetramer and polycondensation products (Scheme 16).[134,135]

Table 1. M_4L_6 Tetrahedral Cages Formed with Bispyrazolyl Pyridine Ligands

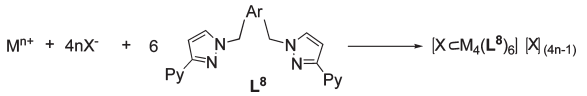

Entry	Ar	Py	Metal	Anion
a			Co(II)	BF_4^- ClO_4^-
b		2-pyridiyl	Zn(II)	BF_4^- ClO_4^-
c	1,2-phenylene	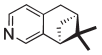 2-pyridyl*	Zn(II)	BF_4^-
d			Co(II)	BF_4^- PF_6^- ClO_4^-
e			Zn(II)	SiF_6^{2-}
f	2,3-naphtalendiyle	2-pyridiyl	Cd(II)	BF_4^-
g	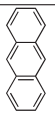		Co(II)	BF_4^-
h	2,3-naphtalenediyl	2-pyridiyl	Zn(II)	BF_4^-
i	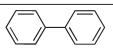 3,3'-biphenylene	 2-pyridiyl	Co(II)	BF_4^- PF_6^- ClO_4^- I^-
j	 1,8-naphtalenediyl	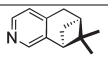 2-pyridyl*	Zn(II)	ClO_4^-

More recently, single-crystal X-ray diffraction carried out on one of the above molecular flasks showed that a 16-electron manganese species $(C_5H_4Me)Mn(CO)_2$ can be trapped (Scheme 17). The latter arises from in situ photodissociation of one encapsulated $(C_5H_4Me)Mn(CO)_3$ complex.[136]

Initially the structure showed the presence of four manganese complexes encapsulated within the cavity of **34**. Upon irradiation of the crystal by 365 nm ultraviolet light at 100 K, the pale yellow crystal becomes greenish-yellow. Successive X-ray analysis showed that one of the encapsulated Mn complexes underwent photodissociation of a carbonyl ligand to give the coordinatively unsaturated $(C_5H_4Me)Mn(CO)_2$ species. The released CO and the 16-electron Mn complex remained trapped within the cavity of **34**. More recently the same group reported the synthesis of a 3D network that results from fused molecular Co_6L_4 capsules that propagate in three axes, via the metal center between two adjacent cages[137] (Figure 13).

Self-assembled molecular cages **34** and **35** possessing a nanometer-sized cavity were used as functional molecular flasks to promote a variety of chemical reactions such as olefin photodimerization, Diels–Alder, cross photoaddition, and [2 + 2]- and [2 + 4]-cycloaddition reactions as illustrated in recent reviews by Fujita and co-workers.[138,139] In these cases, a pair of hydrophobic molecules enters the cavity and the increased concentration and molecular preorganization of reactants within the cage reduce the entropic cost so that acceleration of reactions

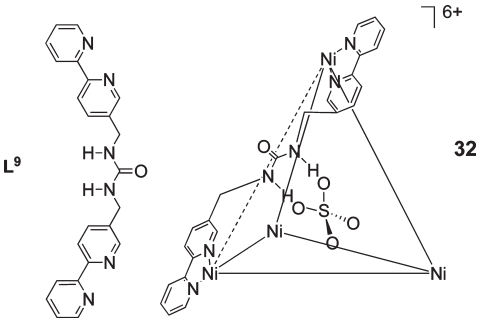

Figure 10. Representation of $\{[SO_4{\subset}Ni_4(\mathbf{L}^9)_6][SO_4]_3\}$ (**32**).

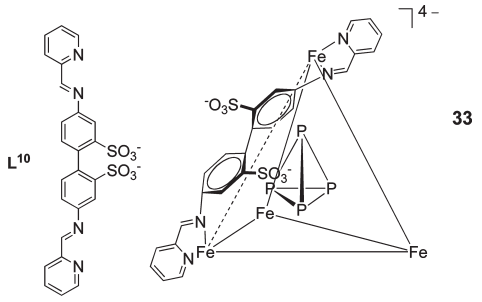

Figure 11. Schematic drawing of ligand $\mathbf{L}^{10}$ and the related tetrahedral assembly encapsulating white phosphorus $\{[P_4{\subset}Fe_4(\mathbf{L}^{10})_6]^{4-}\}$ (**33**).

or even unusual reactions can occur. For example, molecular cage **34** was used to accelerate the room-temperature Diels–Alder reaction of 1,4-naphthoquinone with either cyclohexadiene or 2-methyl-1,3-butadiene. (Scheme 18). The rate of formation of the final product increases, respectively, 21- and 113-fold.[140,141]

The steric restrictions imposed by the rigid well-defined cavity induce favorable arrangement for trapped reactants that could lead to a change in selectivity such as altered regioselectivity. For example, photodimerization of acenaphthylene using the capsule **34** gives exclusively the *syn* dimer, whereas poor selectivity between *syn* and *anti* compounds was observed for the same reaction performed in solution. Surprisingly, the photodimerization of encapsulated 1-methylacenaphthylenes lead only to the formation of the head-to-tail syn isomer, which under normal conditions gives four isomers (Scheme 19).

Similarly, new regioselectivity in confined space was observed for the thermal Diels–Alder reactions of anthracenes with *N*-cyclohexylmaleiimides as dienophile, which instead of giving 9,10-adducts provided 1,4-adducts.[140] Diels–Alder reactions of unreactive naphthalenes and *N*-cyclohexylmaleiimides as dienophiles were also performed with the same capsule **34** where the unexpected 1,4-regioselectivity was obtained[142](Scheme 20).

The above studies show that the confined environment within a cage modifies the selectivities and/or regioselectivities and also that new reactions take place. As a first example, photochemistry of α-diketones and more particularly of benzyl, classically problematic, was described by using the molecular flask **34**.[143] Three unexpected rearrangement products were then obtained in a 4.4/1/2 ratio (Scheme 21). The authors believe that, even under aerobic conditions, traces of O_2 could not be avoided during the reaction course.

In the same way, Fujita and co-workers reported that *ortho*-quinone and sterically hindered toluene, preorganized in the

dx.doi.org/10.1021/cr200345v |*Chem. Rev.* 2012, 112, 2015–2041

Scheme 15. Hierarchies of Host−Guest Inclusion of Coronene, C_{60}, and C_{70} Fullerenes within Host $[Fe_8(Ni{-}L^{11})_6]^{16+}$

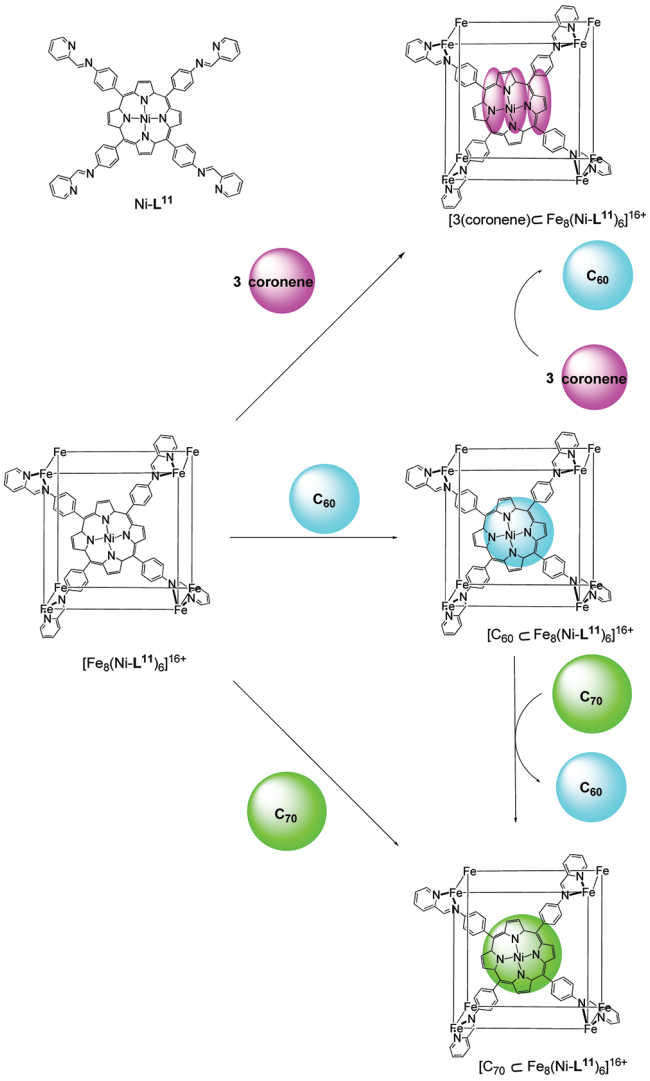

cavity of **34**, are transformed into an unique 1,4-adduct upon photoirradiation despite the difficulties of control in radical reactions[144] (Scheme 22). Upon photoexcitation, recombination of benzylic and semiquinone radicals occurs.

Finally some asymmetric pericylic reactions were realized using chiral cages **36**.[145,146] Indeed the use of *trans-N,N′*-diethylcyclohexanediamine as chiral auxiliary ligand on the Pd(II) centers can be considered for enantiocontrol of the intracavity reactions by formation of a chiral cage possessing the same size and shape characteristics as homologous achiral ones. Thus, the same reactions as those realized within the achiral molecular flask **34** can be envisaged (Scheme 23).

Cross-photoaddition of 3-methylfluoranthene with maleimide occurs with a modest enantioselectivity of 50%. Although these cages make possible the accommodation and then the acceleration and alteration of chemical reactions, the use of an equimolar amount of capsules is necessary to perform the transformations so that examples of assemblies **34** and **35** as catalyst are limited. To make these reactions catalytic, a judicious choice of substrates and also of the host−substrate and host−product are necessary to allow an autoinclusion or an autoexpulsion of the target product. In these transformations described above, the final product is too large to escape through the open faces of the molecular flask.

On the other hand, Fujita and co-workers reported the use of **34** (10 mol %) as phase-transfer catalyst for the Wacker oxidation of styrenes to form the excepted acetophenones because of its high water solubility and its hydrophobic cavity[147] (Scheme 24). This reaction was also extended to linear alkenols and particularly to 8-nonen-1-ol.[148]

The bowl-shaped capsule **35** also showed its efficiency during the Diels−Alder reaction between anthracene and maleimide[140] (Scheme 25). Only 1 mol % of the nanocage was employed, and the reaction was found to be quantitative. The authors suggest that the final product is expelled due to the absence of π-stacking interactions with the host.

The use of coordination assemblies with nanocavities to carry out catalytic transformations within confined spaces has been also investigated by other groups where a catalyst is first encapsulated and activated toward chemical substrates. This strategy will be discussed in the next section.

4.2. M_4L_6 Metallocages with Chiral Vertices As Nanovessels

4.2.1. Design of Chiral M_4L_6 Metallocages. During the past decade, Raymond and co-workers described the self-assembly of a series of chiral M_4L_6 coordination tetrahedra based on the biscatecholate ligands **37**, **38**, and **39** when combined with trivalent metal ions such as Al(III), Ga(III), In(III), Fe(III), and/or tetravalent ions Ti(IV), Sn(IV), and Ge(IV).[149−151] For instance, in the tetrahedral assemblies $[Ga_4(\mathbf{37})_6]^{12-}$, $[Ga_4(\mathbf{38})_6]^{12-}$, and $[Ga_4(\mathbf{39})_6]^{12-}$ (**40**−**42**), each Ga(III) center acquires an octahedral geometry and is chelated by three catecholate arms of the bistetradentate ligands that form the six edges of the tetrahedron (Scheme 26). Furthermore, the chirality established at one vertex is transmitted to the other three centers via the rigid backbones of the bridging ligands, resulting exclusively in homochiral arrangement ($\Delta\Delta\Delta\Delta$ or $\Lambda\Lambda\Lambda\Lambda$). These coordination tetrahedra featured nanosized cavities (0.35−0.5 nm^3) appropriate to encapsulate tetraalkylammonium ions NR_4^+ (R = −Me, −Et, and −Pr). It is worth mentioning that the formation of **40** occurred with or without a guest molecule in the cavity; however, **41** and **42** were only formed in the presence of NMe_4^+ and NEt_4^+ as thermodynamic templates to ensure their formation. In the absence of the guest template, for example, ligand **38** provides the triple-stranded helicate **43**.

The configurational stability of the resolved chiral tetrahedron **40** was investigated in solution by ^1H NMR spectroscopy. Remarkably, the assembly retained its configuration for at least 8 months even in boiling alkaline solution. The authors attribute this high configurational stability of the assembly to the "mechanical stiffness" that arises from the interconnection of the four metal centers through rigid bridging ligands to form a three-dimensional tetrahedral arrangement. This result prompted the authors to use these supramolecular assemblies as nanovessels to carry out enantioselective reactions (vide infra).[7]

On the other hand, Albrecht and co-workers constructed an enantiopure metallosupramolecular complex of type M_4L_4. The chiral tetrahedron was obtained from triangular triscatechol ligand LH6 with enantiomerically pure terminal amide groups and TiO(acac)$_2$ in the presence of alkali metal carbonate to give the tetranuclear titanium(IV) complexes $X_8[Ti_4L_4]$ (X = Li, Na, K). The authors found that the (*S*)-phenylethylamide induces

dx.doi.org/10.1021/cr200345v |*Chem. Rev.* 2012, 112, 2015–2041

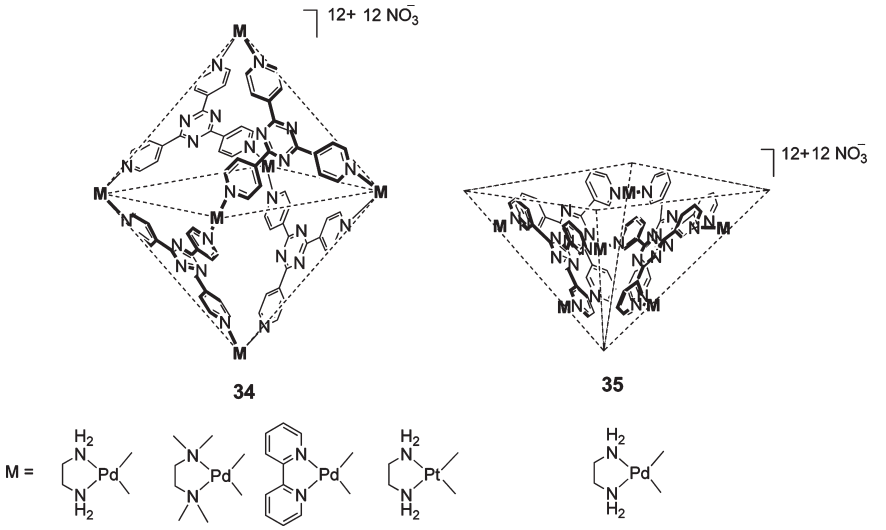

Figure 12. Octahedral cage **34** and the pyramidal bowl-shaped **35**.

Scheme 16. Polycondensation of Trialkoxysilanes Using 34 and 35 Molecular Flasks

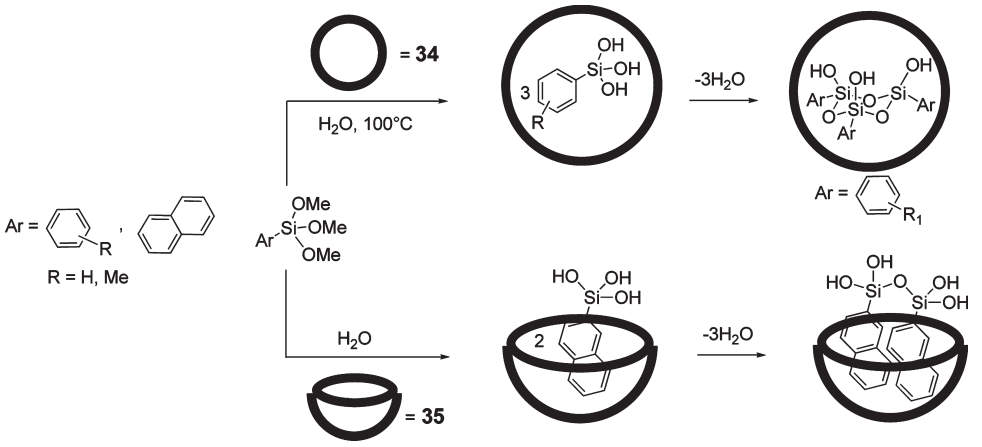

Scheme 17. Stabilization of Reactive Species $(C_5H_4Me)Mn(CO)_2$ within the Cavity of 34

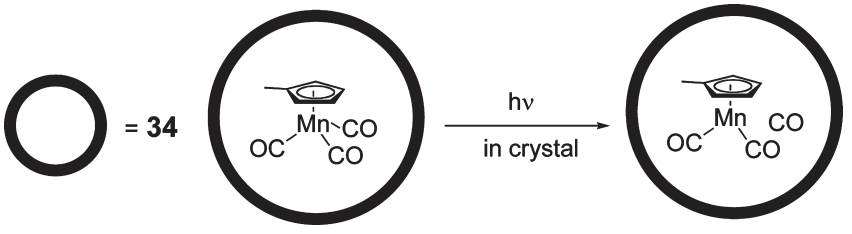

Λ-configuration at the metal centers that transfer the chiral information from outside of the tetrahedron to the interior.[152] Further investigations carried out by the same group allowed the preparation of related tetranuclear $Na_8[Ti_4L'_4]$ where L′ is an ester-substituted triscatecholate ligand. These studies aim to modify the interior of the cavity of the tetrahedron by attachment of a functional group (Figure 14).[153]

Cui and co-workers developed a diastereoselective approach to prepare enantiopure M_4L_6-type nanocapsules. The method consists of preparing an enantiopure atropisomeric ligand LH2 with 1,1′-biphenyl backbone to which two groups of diketones were attached (see Figure 15). Upon treatment of LH2 with MCl_3 (M = Fe, Ga), the desired tetrahedral cages M_4L_6 were obtained and characterized by spectroscopic data and single-crystal X-ray diffraction. The chirooptical properties were investigated by CD measurements and confirmed the enantiopure character of the tetrahedral assemblies. The authors found that starting with chiral (*S*)-L provided the homochiral

dx.doi.org/10.1021/cr200345v |*Chem. Rev.* 2012, 112, 2015–2041

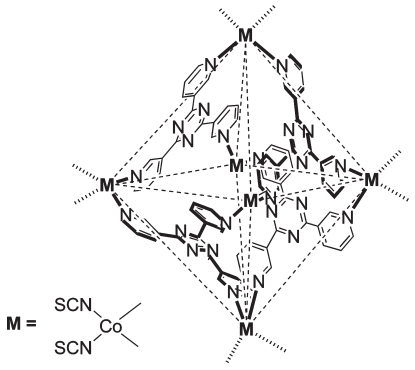

Figure 13. Molecular Co_6L_4 capsule 3D network.

Scheme 18. Diels–Alder Reactions Accelerated within 34

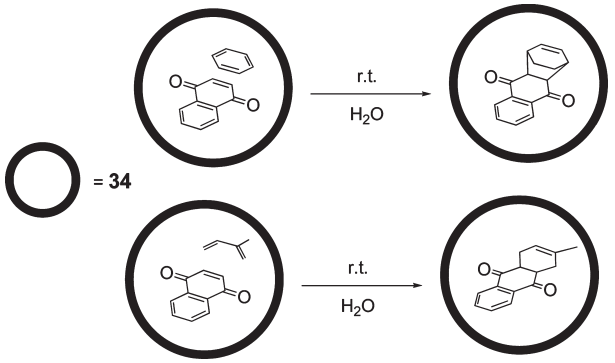

Scheme 19. Photodimerization of Acenaphthylenes within 34

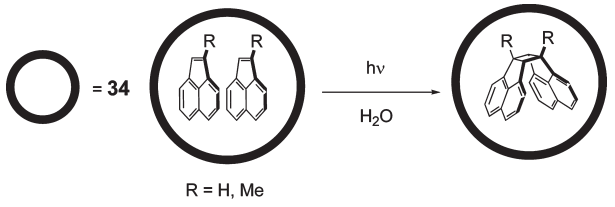

Scheme 20. Diels–Alder Reaction of Unreactive Naphthalenes within 34

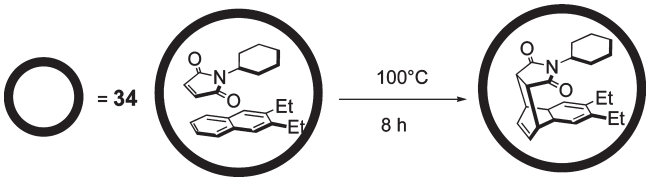

ΛΛΛΛ-M_4L_6 nanocapsule (Figure 15). Furthermore, the nanocapsules were highly efficient for the resolution of racemic alcohols by inclusion during crystallization; for example, the (*S*)-2-butanol was included with enantiomeric excess (ee) value of 98.8% based on gas chromatograph (GC) analysis.[154]

More recently, the group extended this approach toward the preparation of homochiral micro- and mesoporous MOFs from predesigned heptanuclear triple-stranded helicate $[Cu_7(OH)_2L_3]$ subunits where L is now an enantiopure hexadentate tetranionic ligand with 1,1′-biphenyl backbone but bearing two pyridine functionalized Schiff base units to promote the preparation of the hierarchical 3D chiral networks.[155]

4.2.2. Catalysis in Supramolecular Media Using Chiral M_4L_6 Capsule. As presented in the previous section, the chiral self-assembled M_4L_6 supramolecular tetrahedron can encapsulate a variety of tetra-alkyl ammonium guests and presents high configurational stability. Raymond, Bergman, and co-workers used the tetrahedral $[Ga_4(\mathbf{37})_6]^{12-}$ (**40**) (H4(**37**) = 1,5-bis(2,3-dihydroxybenzamido)naphthalene) (Figure 16) as a host to encapsulate reactive cationic organometallic complexes and studied some catalytic transformations within the chiral environment of the cavity of the supramolecular tetrahedron.

The preparation of the desired host–guest complexes $[M\subset Ga_4L_6]^{11-}$ was quantitative upon exchanging the weakly encapsulated NMe_4^+ in the starting material $[NMe_4\subset Ga_4(\mathbf{37})_6]^{11-}$ by the cationic organometallic complex "M". The generation of the host–guest complexes $[M\subset Ga_4(\mathbf{37})_6]^{11-}$ was easily observed by ^{1}H NMR spectroscopy. The resonances of the encapsulated guest are shifted significantly upfield due to shielding of the naphthalene moiety of the host assembly, illustrating the close contact between host and guest. Following the above procedure, a variety of organometallic guests such as Cp_2Fe^+, Cp_2Co^+, $[CpRu(p\text{-cymene})]^+$, CpRu(diene)X, Cp*Ru(diene)X, $[Cp^*Ir(PMe_3)(Me)(C_2H_4)]^+$, and other related systems were encapsulated in the tetrahedral assembly $[Ga_4L_6]$.[12,17]

Upon encapsulation of chiral organometallic complexes such as $[Cp^*Ru(CH_2{=}CH{-}CHR^1{=}CHR^2)(H_2O)]^+$ in the chiral tetrahedral assembly $[Ga_4L_6]^{12-}$, four different host–guest stereoisomers are formed (Δ/R, Δ/S, Λ/R, Λ/S), i.e., two diastereomeric pairs of enantiomers. The ratio of the diastereomers varied from 52:48 up to 85:15 depending on the substituents R^1 and R^2 of the diene moiety.[157] Although the diastereomeric ratios are modest compared to those available by conventional reagents, the chiral recognition here relies only on weak van der Waals interactions. These results compared well with other diastereomeric ratios obtained in host–guest systems.[158]

Most interesting was the use of the chiral tetrahedral assembly $[Ga_4(\mathbf{37})_6]^{12-}$ (**40**) as a nanosized reaction vessel to carry out C–H activation reaction by encapsulated iridium complex. Combination of $Na_{12}[Ga_4(\mathbf{37})_6]$ with $Cp^*Ir(PMe_3)(Me)(CH_2{=}CH_2)$ resulted in the immediate and quantitative encapsulation to form $Na_{12}[Cp^*Ir(PMe_3)(Me)(CH_2{=}CH_2)\subset Ga_4(\mathbf{37})_6]$. The corresponding host–guest assembly displayed C–H bond activation at elevated temperature in the presence of an aldehyde. The new products were identified as the host–guest assembly $[Cp^*(PMe_3)Ir(R)(CO)\subset Ga_4(\mathbf{37})_6]^{11-}$ from the C–H activation of the aldehyde substrates used in the reaction.[159,160]

Interestingly, the C–H activation results obtained with the host–guest assembly were different than those obtained from the same reaction but using the free iridium catalyst $Cp^*Ir(PMe_3)(Me)(CH_2{=}CH_2)$. For example, experiments conducted in the absence of $[Ga_4(\mathbf{37})_6]^{12-}$ (**40**) host demonstrated that the free catalyst $Cp^*Ir(PMe_3)(Me)(CH_2{=}CH_2)$ reacts with all of the aldehydes shown in Table 2 at similar rates, whereas the host guest assembly $Na_{12}[Cp^*Ir(PMe_3)(Me)(CH_2{=}CH_2)\subset Ga_4(\mathbf{37})_6]$ strictly regulates the ability of the aldehyde substrates to react with the iridium center based on their size and shape. Large aldehydes such as benzaldehyde and pivalaldehyde are too bulky to enter the host cavity, whereas

Scheme 21. Photodimerization α-Diketones within 34

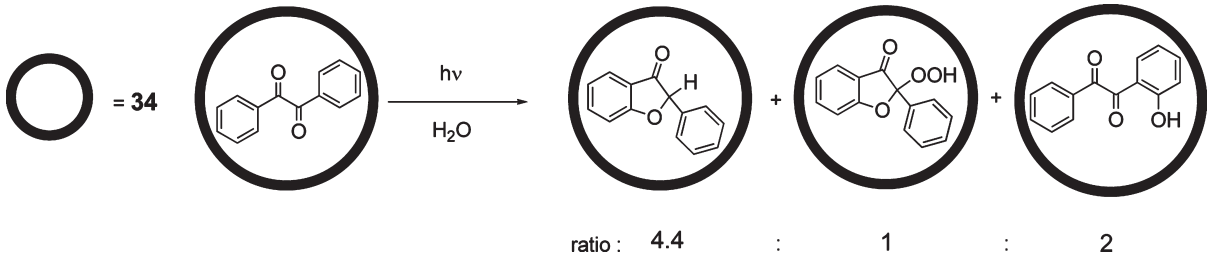

Scheme 22. Photochemistry of *ortho*-Quinone and a Benzylic Substrate within 34

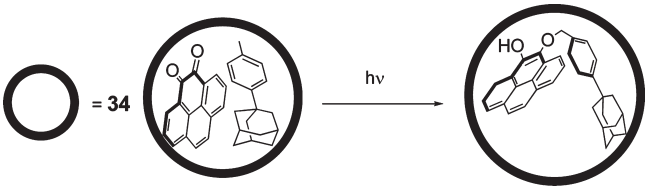

Scheme 23. Asymmetric Pericyclic Reactions within 36

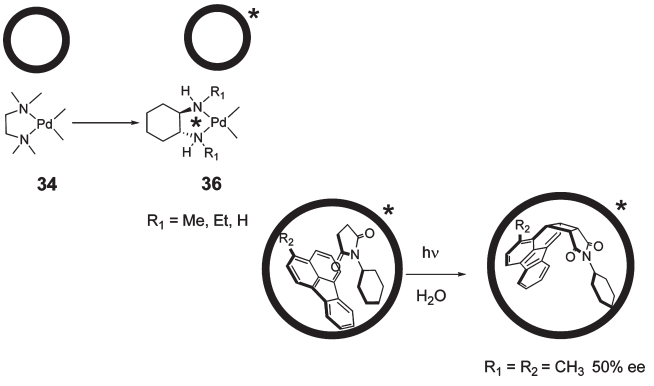

Scheme 24. Use of 34 as Phase-Transfer Catalyst

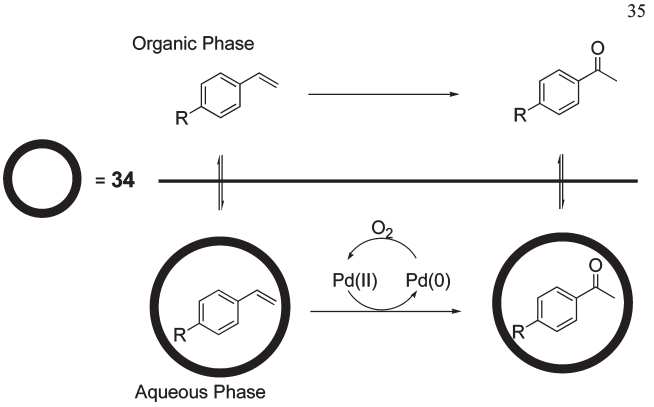

smaller aldehydes are readily activated since they are able to interact with the encapsulated complex Cp*Ir(PMe_3)(Me)-(CH_2═CH_2). Because of this contrast between the free catalyst

Scheme 25. Use of 35 as Catalyst

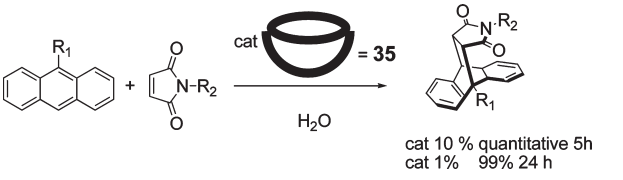

Scheme 26. Preparation of a Series of M_4L_6 Tetrahedra

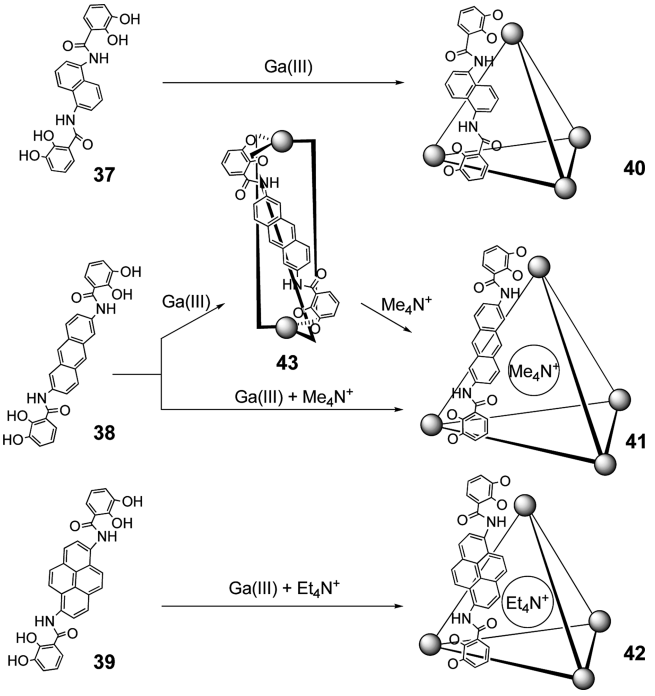

behavior and the host−guest system, it is concluded that the C−H bond-activation reaction takes place within the host assembly (Table 2).[7] Because of product inhibition, the C−H activation by this host−guest system could not be used in a catalytic fashion with turnover numbers.

On the other hand, Raymond, Bergman, and co-workers used the chiral tetrahedral host $[Ga_4(\mathbf{37})_6]^{12-}$ (**40**) as a catalyst by itself to carry out some catalytic reactions such as 3-aza-Cope rearrangement of enammonium cations to give γ,δ-unsaturated aldehyde products, via formation of imminium cations first and subsequent hydrolysis (Scheme 27).[161] It is noteworthy that in

dx.doi.org/10.1021/cr200345v |*Chem. Rev.* 2012, 112, 2015–2041

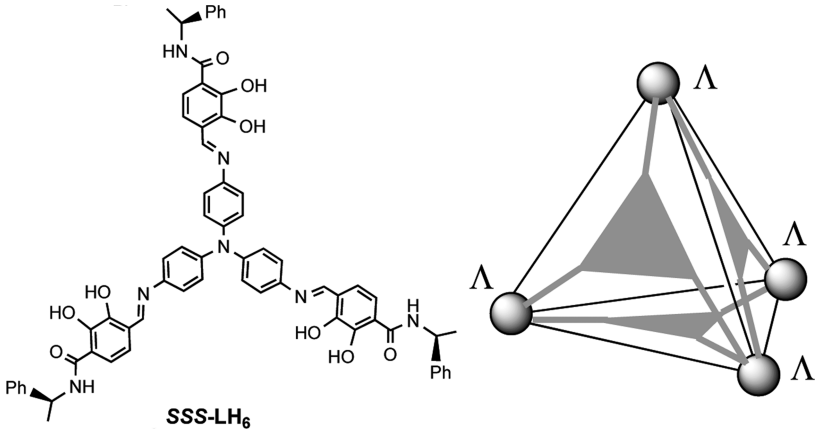

Figure 14. Triangular enantiopure metallosupramolecular complex of type M_4L_4 from chiral triscatechol ligand LH6.

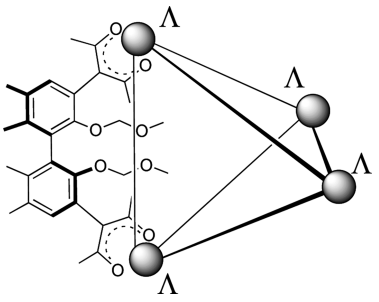

Figure 15. Schematic drawing of ΛΛΛΛ-M_4L_6 (M = Ga, Fe) with enantiopure tetradentate ligand.

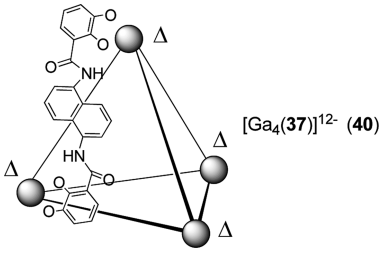

Figure 16. Tetrahedral host $[Ga_4(\mathbf{37})_6]^{12-}$ (**40**).

both reactions the catalytic rate is enhanced up to 1000 times. The enantioselective version of the above reaction was also investigated using the enantiopure tetrahedral host Δ,Δ,Δ,Δ-$[Ga_4(\mathbf{37})_6]$.[12,162]

Furthermore, acid hydrolysis of orthoformates in basic solution was possible (Scheme 28) using the tetrahedral host. The reaction rate was accelerated to 890-fold compared to the uncatalyzed reaction.[163]

Extension to catalytic deprotection of acetals in basic solution using the tetrahedral nanovessel was accomplished successfully as well.[164] It is believed that reaction space restriction inside the capsule **40** as well as preorganization of the substrates into reactive conformations accelerates the catalytic reactions described above. Remarkably the authors have shown that rate enhancement comparable to those seen in enzymatic systems has been achieved using the above assembled host in Nazarov cyclization reaction (Scheme 29). Thus, Nazarov cyclization of 1,4-pentadiene-3-ols to give C_5Me_5H in water and in mixed water/dimethyl sulfoxide (DMSO) occurs at a rate up to 2 100 000 times larger than that of the uncatalyzed reaction.[165] It should be mentioned that the supramolecular catalyst suffers from product inhibition, i.e., the assembled host does not bind the reactant more strongly than it binds the product. To overcome this problem, the authors treated Cp*H with maleimide to give a Diels−Alder adduct that is a noncompetitive guest.

More recently, Raymond, Bergman, Toste, and co-workers reported the encapsulation of some gold−phosphine complexes inside the tetrahedral host (Scheme 30). The authors investigated the catalytic activity of the resulting host−guest assembly $PMe_3Au^+ \subset [Ga_4(\mathbf{37})_6]^{12-}$ for the intramolecular hydroalkoxylation of allenes. The catalytic activity of the encapsulated gold complex was enhanced 8-fold compared to the classical procedure with the gold complex alone.[166]

The importance of this field prompted chemists to develop other approaches based on coordination assemblies that hold promise for the development of artificial enzymes. These studies are presented in the next section.

4.3. Other Coordination Assemblies That Mimic Enzyme Functionalities

Unlike the previous examples where the confined spaces or cavities of the molecular flasks are used to promote chemical transformations or via loose encapsulation of active catalysts to enhance the catalytic activities, in this section we present another approach where the active catalyst is a part of the supramolecular assembly or at least strongly bound inside the cavity of the overall framework and around which inactive metal complexes are linked and act as fences or walls (a) to protect the catalyst active site, (b) to increase its stability and lifetime, and ultimately (c) to modify its reactivity by taking advantage of the cavity size for selective encapsulation of the reactants. To this end, the groups of Hupp and Nguyen attached the active catalyst, a bispyridyl Mn(III)porphyrin epoxidation catalyst, inside the cavity of a molecular square. The latter is formed of $[Re(CO)_3Cl]$ corners and four inactive Zn(II) porphyrins that act as walls of the supramolecular assembly (see Scheme 31).[167]

The authors have found that placement of the active Mn-porphyrin inside the cavity of the molecular square increases the stability of the catalyst by impeding the process of formation of the oxo-bridged manganese dimer (Mn−O−Mn) responsible for the catalyst deactivation. Moreover, during the epoxidation of styrene, the activity of the catalyst is enhanced 10-fold and the lifetime is increased to 3 h compared to the free Mn-porphyrin

dx.doi.org/10.1021/cr200345v |*Chem. Rev.* 2012, 112, 2015–2041

Table 2. C−H Bond Activation of Aldehydes Using $Na_{12}[Cp^*Ir(PMe_3)(Me)(CH_2{=}CH_2) \subset Ga_4(37)_6]$

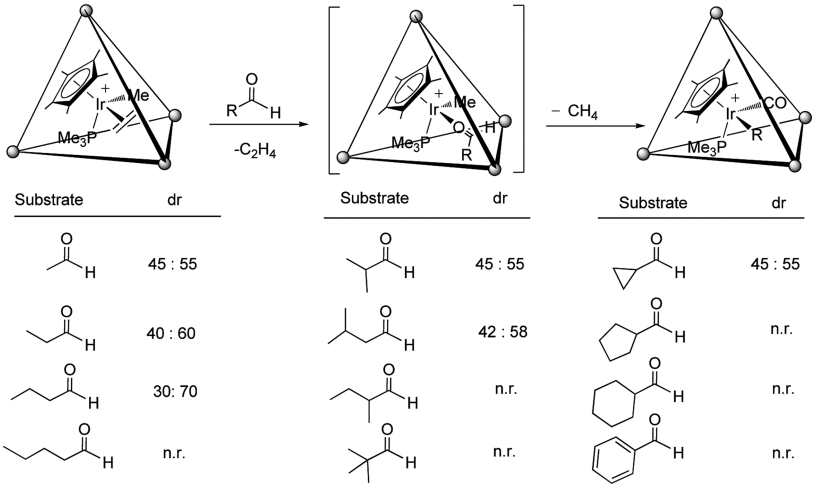

Scheme 27. Catalytic Cycle of the aza-Cope Rearrangement Using 40

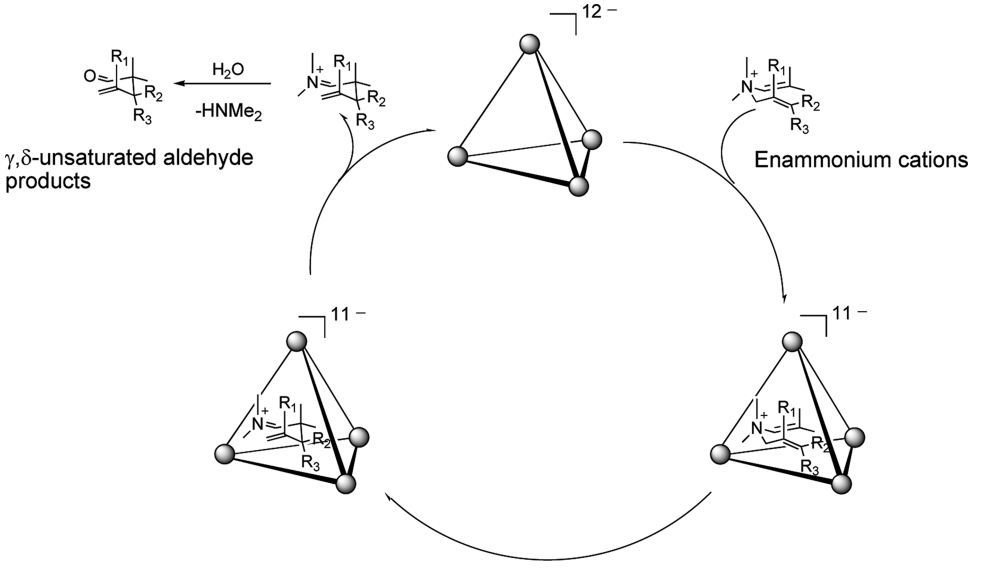

complex, which lasts only 10 min. Furthermore the selectivity of the bound Mn-porphyrin catalyst is also modified relative to the free catalyst. For instance, competitive epoxidation of both the sterically demanding substrate *cis*-3,3′,5,5′-tetra(terbutyl)stilbene (**44**) and *cis*-stilbene showed that the catalyst activity is 3.5 times less reactive with Mn−Zn4 supramolecular assembly for the more encumbered substrate **44** compared to the free Mn catalyst. This behavior is no doubt related to the size of cavity of the supramolecular assembly, which controls the selectivity of substrate epoxidation.[167] The authors have also demonstrated that, upon reducing the size of the cavity by introducing two coordinating ligands (3,5-dinicotinic acid dineomenthyl ester), the epoxidation of **44** relative to the smaller substrate is now 7 times less with the supramolecular assembly than with the naked catalyst.

Hupp, Nguyen, and co-workers pushed this approach further and constructed a rigid rectangular box composed of 18 porphyrin metalated units (Scheme 32).[168] This coordination

Scheme 28. Acid Hydrolysis of Orthoformates in Basic Solution Using 40

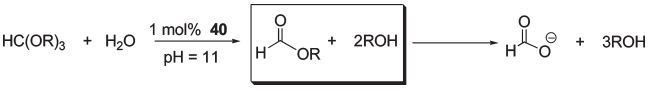

assembly consists of four Zn-porphyrin trimers (T) and two Sn(IV) porphyrin dimers (achiral "A" or chiral "C") that act as edges of the rectangular box while the active catalyst Mn-porphrin dimer (M) is placed inside the cavity of the box in the hopes to increase the rigidity of the overall framework $AMAT_4$ for applications in epoxidation of olefins or with $CMCT_4$, the chiral version for enantioselective oxidation. These complex architectures were characterized by solution-phase X-ray scattering and fluorescence spectroscopy.

dx.doi.org/10.1021/cr200345v |*Chem. Rev.* 2012, 112, 2015–2041

The $AMAT_4$ supramolecular boxes showed size selectivity toward oxidation of *cis*-stilbene, which was found to be 5.5-fold more reactive than the sterically hindered *cis*-3,3′,5,5′-tetra(*tert*-butyl)stilbene (**44**).[169] When the chiral supramolecular assembly $CMCT_4$ was employed for the enatioselective oxidation of *p*-tolylsulfide, the related methyl tolyl sulfoxide was obtained with only 12% ee whereas the free catalyst showed no enantioselectivity. Here an achiral Mn-porphyrin catalyst is employed but the chiral information carried by Sn(IV)porphyrin is transmitted through the supramolecular assembly to the substrate during oxidation. When *N*-acetyl-(L)-phenylalanine was employed instead of the (D)-counterpart, the sense of the chiral excess was reversed.

Mirkin and co-workers carried out further investigations in this area. The authors developed the synthesis of coordination assemblies that mimic enzyme functionalities based on metallomacrocycles where an active salen-based catalyst is attached. The preparation of these supramolecular assemblies is based on the weak link approach (WLA). As a consequence, the coordination assembly acquires two different modes, either opened structure where the system becomes active or closed structure where the system becomes inactive. This modification takes place via an

Scheme 29. Acid-Catalyzed Nazarov Reaction of Pentadienols to Give Cylopentadiens within the Assembled Cage 40

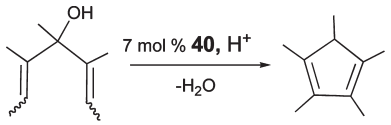

Scheme 30. Intramolecular Hydroalkoxylation of Allenes Mediated by Encapsulated Gold Complex

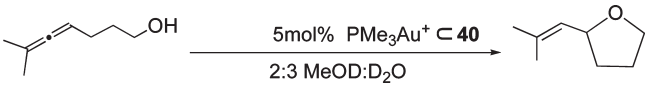

Scheme 31. Placement of the Active Mn(III)-Epoxidation Catalyst Inside the Cavity of a Molecular Square, Re = $[Re(CO)_3Cl]$

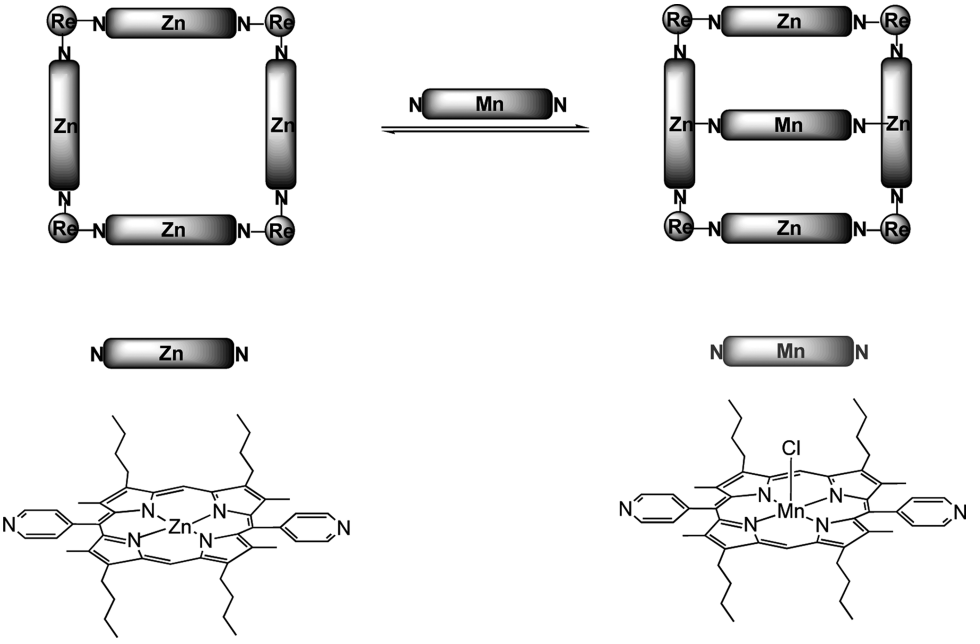

Scheme 32. Rigid Rectangular Box Assembled From 18 Metalated Porphyrins for Oxidation of Olefins

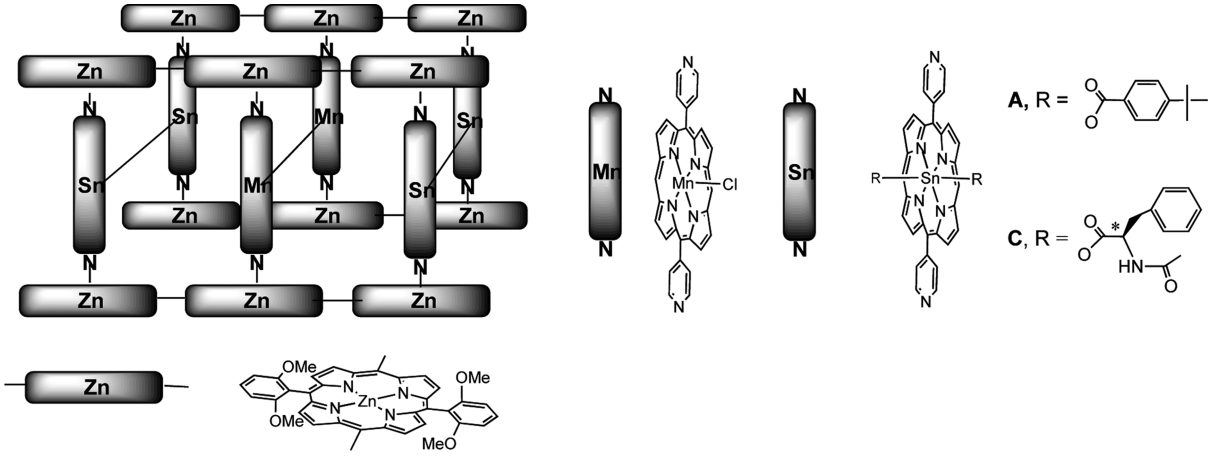

dx.doi.org/10.1021/cr200345v |*Chem. Rev.* 2012, 112, 2015–2041

Scheme 33. Metalated Macrocycles with Active Zn(II) and Cr(III) Catalysts (Closed mode: catalyst A: M^1 = Rh, M^2 = Cr^{III}−Cl, n = 2, Y = BF_4; catalyst A: M^1 = Rh, M^2 = Zn^{II}, n = 2, Y = BF_4; catalyst B: M^1 = Rh, n = 2, Y = BF_4; catalyst C: M^1 = Rh, n= 6, Y = BF_4/OAc; Opened mode: catalyst A: M^1 = Rh, M^2 = Cr^{III}−Cl, L^1/L^2 = Cl/CO, n = 0; catalyst B: M^1 = Rh, L^1/L^2 = Cl/CO, n = 0; catalyst C: M^1 = Rh, L^1/L^2 = Cl/CO, n = 4, Y = BF_4/OAc; catalyst A: M^1 = Rh, M^2 = Zn^{II}, L^1/L^2 = OAc/CO, n = 0)

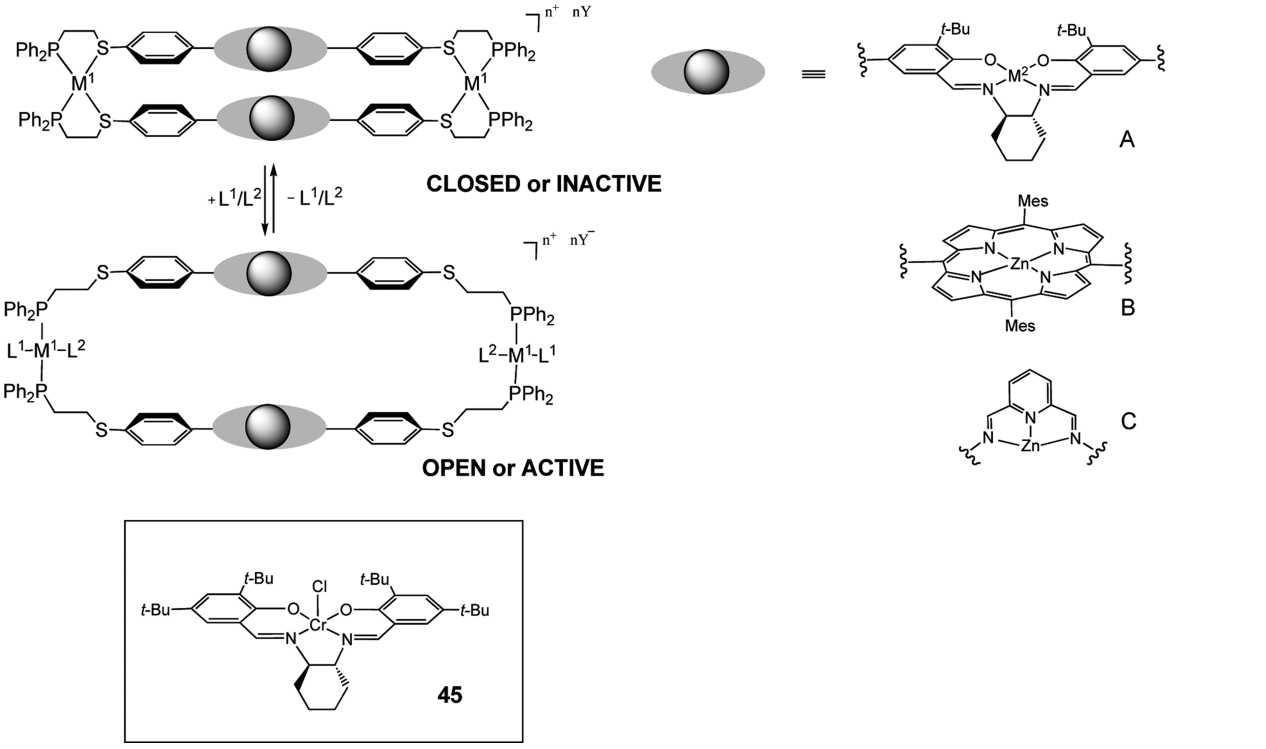

external stimulus, which in this case is weakly coordinated anions or ligands. The authors define such a trend as ion-induced allosteric regulation in relevance to enzyme behavior. For further information the reader may consult a recent review published by the authors.[9]

To this end, Zn(II) and Cr(III) active catalysts were introduced into macrocycles following the weak link approach to give a complex architecture (Scheme 33). The latter can exist in two forms, either open (or active) or closed (or inactive) via combined addition of CO and chloride anions (Scheme 33). This process can be done in a reversible manner.

The Rh−Cr(III) supramolecular catalyst was two times faster when it is in the open state than in the closed state for asymmetric ring-opening of cyclohexene oxide **46** with trimethylsilyl azide to give azide. Furthermore, an ee of 68% was observed in the closed state, which is higher than that of the free Jacobsen catalyst **45**, which under the same conditions showed a 12% ee.[170]

A more contrasting behavior between open and closed states was observed when the Rh−Zn(II) salen catalyst was used for the catalytic acyl transfer reaction between 4-pyridylcarbinol **47** and acetic anhydride **48** (Scheme 34).[171] Indeed the rate was enhanced 25 times in the open state compared to the less active closed state. The Rh−Zn(II) porphyrin systems were also prepared in which the metallomacrocycle is in open or in closed fashion. Acyl transfer reactions from acetylimidazole **49** to 2-, 3-, and 4-pyridylcarbinol isomers were investigated by these catalysts (open and closed) (Scheme 34).[172] As expected rates increased from closed to open, however, isomer discrimination effect was also noticed. In fact, no increase in catalytic rate was

Scheme 34. Various Reactions Catalyzed by the Previous Supramolecular Catalysts in Open and Closed Forms

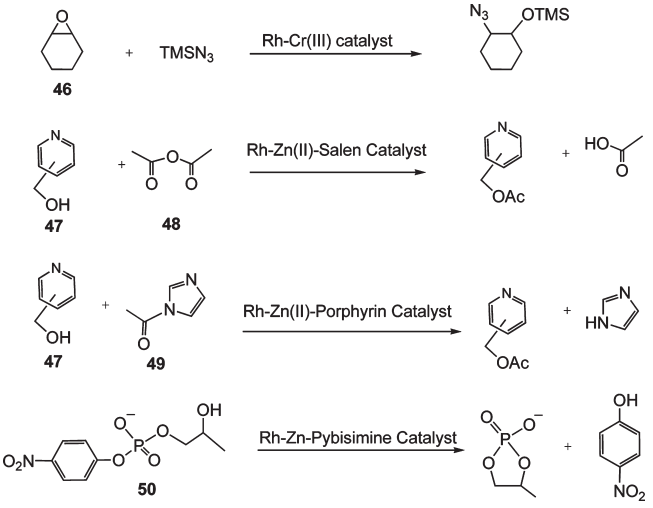

obtained with 2-pyridylcarbinol (whether open or closed or with free catalyst). These results suggest substrate selectivity reminiscent to behavior of enzyme pocket functionality.

More interesting was the example of Rh−Zn(II) pyridine bisimine catalyst, which could be assembled in open and closed macrocycle.[173] The X-ray molecular structure of the closed state showed that the two Zn(II) centers are bridged by an acetate anion, which eventually would hamper substrate access to Zn(II)

dx.doi.org/10.1021/cr200345v |*Chem. Rev.* 2012, 112, 2015–2041

sites. As a result, no catalytic activity was observed. Opening the inactive complex with CO/Cl^- led to high active catalyst resulting in quantitative phosphodiester cleavage of **50** within 40 min (Scheme 34).

On the other hand, the group has also prepared related systems based on Cr(III) salen catalysts defined as "tweezer catalysts", which also were assembled in opened and closed fashion (Scheme 35).[9,174] Their catalytic behavior showed dependence to whether the tweezers are opened (trans) or closed (cis). Unlike the previous system, the closed rigid state showed a 2-fold rate enhancement compared to the open state in the catalytic ring-opening of cyclohexene oxide with $TMSN_3$.

Further investigations were carried out to prepare self-assembled capsules that mimic enzyme functionalities and in which the catalyst active center is firmly bound inside the cavity of the nanocapsule through metal−ligand interactions. Thus, Reek and co-workers developed a novel type of nanocapsule by using a different approach defined by the author as "ligand−template approach".[8,175,176] The template ligands are mainly trispyridylphosphino ligands $P(Py)_3$ and are tetradentate (Scheme 36). The three pyridyl units bind three Zn(porphyrin) moieties to construct the nanocapsule assembly whereas the phosphino ligand will coordinate to the active metal catalyst inside the cavity (M = Rh, Pd). These nanoreactors were used as catalysts to study the hydroformylation of alkenes.

Indeed nanocapsule *m*-Rh−Zn3 based on three Zn(porphyrin), Rh(CO)(acac) as catalyst precursor and templated by tris(*meta*-pyridyl)phospine ligand P(*m*-Py)$_3$ was used in the hydroformylation of 1-octene.[177] The results show that the *m*-Rh−Zn3 system is 10-fold more active than nonencapsulated catalyst $HRh(CO)_2(P(m\text{-}Py)_3)_2$. In addition, the selectivity for the product is reversed; the supramolecular catalyst provided 63% of branched aldehyde compared to 26% observed with the nonencapsulated catalyst $HRh(CO)_2(P(m\text{-}Py)_3)_2$. On the other hand, when the template ligand tris(*meta*-pyridyl)phospine P(*m*-Py)$_3$ was replaced by the less-hindered tris(*para*-pyridyl)phospine ligand P(*p*-Py)$_3$, the related nanocapsule *p*−Rh-Zn3 showed different selectivity in the hydroformylation of 1-octene by providing the linear aldehyde as the major product in a similar fashion to that observed with the free rhodium catalyst $HRh(CO)_2(P(p\text{-}Py)_3)_2$. The authors explain these results by the fact that the *p*-RhZn3 nanocapsule display a more open structure relative to the *m*-RhZn3 system. Consequently, it favors the formation of the bisphosphine active Rh-catalyst, as is the case with the nonencapsulated catalyst $HRh(CO)_2(P(p\text{-}Py)_3)_2$.[177]

On the other hand, when the *m*-RhZn3 system was used in the hydroformylation of 2-octene, 2-ethyloheptanal was obtained in 88% yield, whereas the free catalyst gives a near statistical mixture of 2-methyloctanal and 2-ethyl heptanal[178] where the change in selectivity is attributed to the confined nanospace of the *m*-RhZn3 catalyst system.

Very recently, Reek, Berthon-Gelloz, and co-workers constructed a Rh−Zn2 supramolecular catalyst but this time templated with a chiral (*S*)-4-pyridylphosphoramidite tridentate ligand (Scheme 37). In situ high-pressure ^1H and ^{31}P NMR spectroscopic data and infrared spectroscopy carried out under hydroformylation conditions suggest that the bulky phosphine ligand occupies an axial position

Scheme 35. Tweezer-type Salen-Based Catalysts

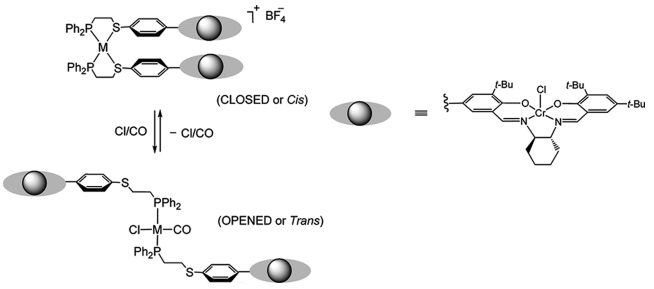

Scheme 36. Nanoreactors (*m*, *p*)-Rh−Zn3 and Their Use As Catalysts in the Hydroformylation of 1-Octene

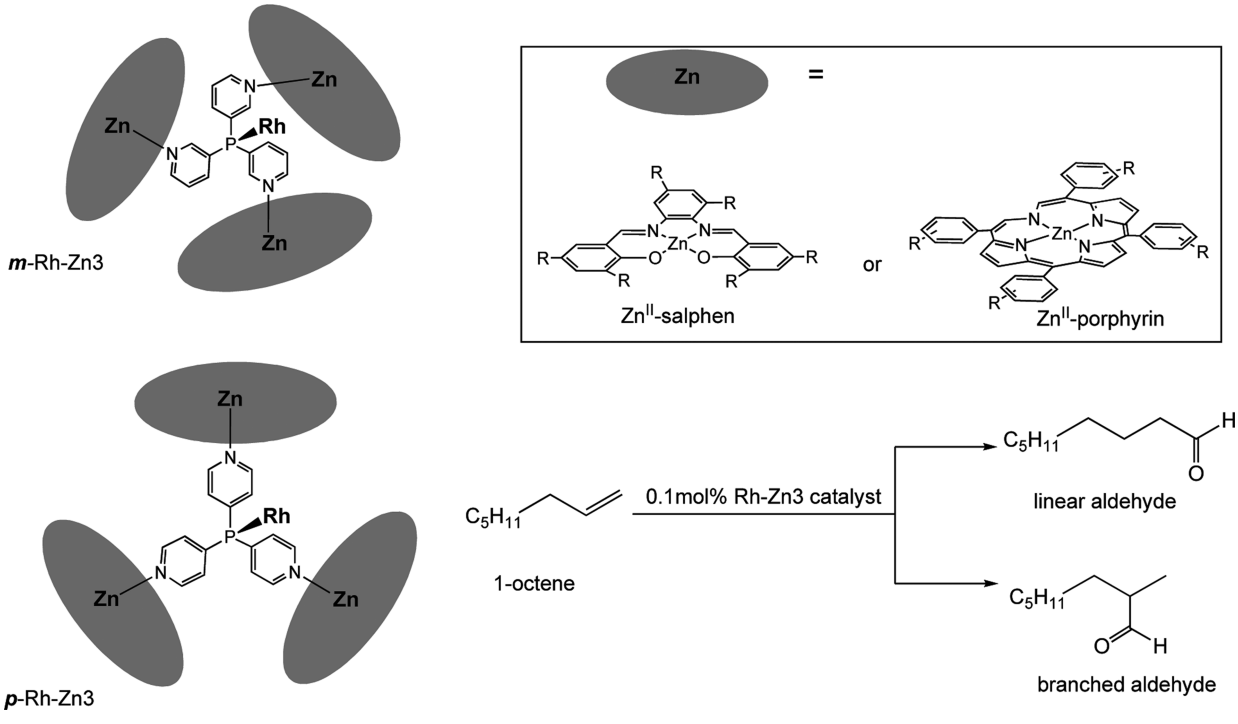

dx.doi.org/10.1021/cr200345v |*Chem. Rev.* 2012, 112, 2015–2041

Scheme 37. Rh−Zn2 Supramolecular Catalyst Templated with a Chiral Tridentate Ligand

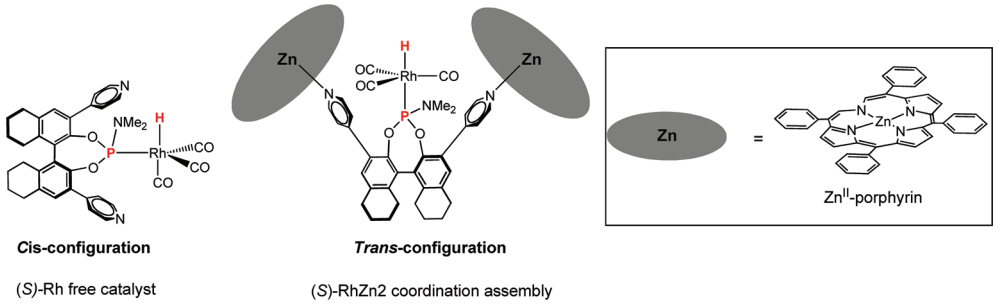

and is *trans* to the hydride, which is in contrast to free catalysts where phosphines normally occupy the equatorial positions.[179] This unusual coordination mode in Rh−Zn2 is facilitated by a supramolecular control imparted from the Zn(II)porphyrin units.

The catalytic properties of the supramolecular catalyst Rh−Zn2 were investigated toward the hydroformylation of 2-octene. Remarkably the results show that the Rh−Zn2 system exhibited a higher conversion (54%) and enantioselectivity (45%) compared to the free catalyst with only 12% conversion and 25% ee. These results illustrate the positive effect in hydroformylation catalysis imparted from the confined space in the supramolecular coordination assembly RhZn2.

5. OUTLOOK AND PERSPECTIVES

In this review, we demonstrated through many examples that coordination assemblies with well-defined cavities could be used as molecular containers to encapsulate a variety of guests. The range of guests includes anions, in particular weakly coordinated ones that can move freely in and out of the cavities, to aromatic molecules such as anthracene and coronene that can be stabilized inside the cavities through $\pi-\pi$ interactions, to the more-challenging encapsulation of the large C_{60} and C_{70} fullerenes. Perhaps the most exciting application of these molecular flasks, demonstrated more recently, is their ability to allow catalytic transformations to occur despite the fact that supramolecular catalysts suffer from product inhibition and require relatively large catalyst loading. The confined spaces in these molecular flasks are thought to induce substrate preorganization, which in turn promotes higher or reversed selectivity and increased reaction rate compared to reactions under conventional conditions. In general, the challenge to the field is to engineer a system that produces significant changes in selectivity, taking into account the many factors or interactions that may be reinforcing each other or may compete. Perhaps the most exceptional example to date is the ability of the host $[Ga_4(\mathbf{37})_6]^{12-}$ (**40**) to speed Nazarov cyclization of 1,4-pentadiene-3-ols to give C_5Me_5H in water and mixed water/DMSO by up to 2 100 000 times, an enhancement resembling those seen in enzymatic systems. This and many other results summarized in this review hold promise for future development in the area of supramolecular catalysis.

Furthermore, it has been also shown that the active catalyst can be firmly encapsulated within the cavity or is a part of the overall framework. In such a situation, the active center is surrounded by other metal complexes, which act as fences or walls to protect the catalyst; moreover, the active metal center takes advantage of the confined space to perform unique types of transformations. Indeed, this approach has recently been introduced in the design of metal−organic frameworks (MOFs) with functionalized pores; for instance, Yaghi, Oisaki, and co-workers used active metal catalyst as part of bridging ligands that can be further transported into MOFs in the presence of Zn_4O as nodes.[180] On the other hand, Champness, George, and co-workers constructed photoreactive MOFs by using M(diimine dicarboxylate)$(CO)_3X$ chromophores as struts and MX_2 as nodes (M = Mn or Re; X = Cl or Br).[181] In this example, the chromophore is now a part of the overall metal−organic frameworks. Surprisingly, the nature of the exited state is modified from ^{3}MLCT in the initial complex to $\pi-\pi^*$ in the MOF environment.

All in all, one would expect that coordination-driven self-assembly will continue to be an active area where a variety of functional assemblies with nanocavities will be prepared and the properties of their confined spaces are awaiting to be unraveled. The design of such future molecular flasks is only limited by the boundless imagination of synthetic coordination chemists.

AUTHOR INFORMATION

Corresponding Author

*E-mail: hani.amouri@upmc.fr.

BIOGRAPHIES

Hani, Haniel Amouri, was born in Anapolis Goias (Brazil) and obtained his Ph.D. degree (1987) in chemistry from Université Louis Pasteur Strasbourg (France), with Professor John A. Osborn, on the subject of homogeneous catalysis (hydrogenation). In 1988 he spent one year at Gif-sur-Yvette (France) as a postdoctoral fellow with Dr. Hugh Felkin, and he studied C−H activation of saturated hydrocarbon with transition metal

polyhydrides. In 1992−1993 he spent one year at UC—Berkeley (USA) with Professor K. Peter C. Vollhardt and was working on the synthesis of oligocyclopentadienyl metal complexes and their behavior as electron-transfer reagents. He is a Research Director in CNRS and is currently the director of the "ARC" group (Autoassemblage, Reconnaissance et Chiralité) at Université Pierre et Marie Curie Paris-6. His main research interests are chirality and organometallic and supramolecular coordination chemistry. He has over 100 research papers and reviews published in international scientific journals and is one of the authors of the book *Chirality in Transition Metal Chemistry* published by Wiley in 2008.

Christophe Desmarets was born in Saint-Avold (France) and obtained his Ph.D degree (2003) in chemistry from University of Nancy I with Professor Y. Fort on the subject of nickel-catalyzed polyarylamines synthesis for the development of material conductors. In 2004 he spent 18 months as a postdoctoral fellow (Alexander von Humbolt) with Professor John A. Gladysz at Erlangen—Nürnberg where he studied the synthesis of triangular platinum complexes with carbon chain linkages. In 2006 he joined the group of Dr. H. Amouri as maître de conférences and started working on the preparation of coordination assemblies for host−guest chemistry.

Jamal Moussa was born in Oulad el Bali (Morocco) and obtained his Ph.D in 2007 from Université Pierre et Marie Curie, Paris, under the supervision of Dr. H. Amouri working on luminescent materials based on organometallic linkers. He then joined the ETH Zürich, Switzerland, for two years as a postdoctoral fellow with Professor Antonio Togni where he worked on Ni(II) asymmetric catalytic hydroamination and [2 + 3]-dipolar cycloaddition reactions of unsaturated nitriles using phosphane and NHC-based chiral ferrocenyl ligands. In 2009 he joined the group of Dr. H. Amouri as maître de conférences and started working on the design of late transition polymetallic assemblies for applications in the field of luminescence and catalysis.

ACKNOWLEDGMENT

The authors would like to thank UPMC and CNRS for supporting this work. H.A. would like to thank his collaborators, Ph.D. students, and graduate and undergraduate students for their contribution to this research program. H.A. also thanks Lise Marie Chamoreau for helping to draw molecular structures from Cif's files.

REFERENCES

(1) Fujita, M.; Ogura, K. *Coord. Chem. Rev.* **1996**, *148*, 249.
(2) Stang, P. J.; Olenyuk, B. *Acc. Chem. Res.* **1997**, *30*, 502.
(3) Caulder, D. L.; Raymond, K. N. *Acc. Chem. Res.* **1999**, *32*, 975.
(4) Steed, J. W.; Atwood, J. L. *Supramolecular Chemistry, Concept and Perspectives*; Wiley: Chichester, U.K., 2000.
(5) Ward, M. D. *Chem. Commun.* **2009**, 4487.
(6) Han, Y.-F.; Jia, W.-G.; Yu, W.-B.; Jin, G.-X. *Chem. Soc. Rev.* **2009**, *38*, 3419.
(7) Fiedler, D.; Leung, D. H.; Bergman, R. G.; Raymond, K. N. *Acc. Chem. Res.* **2005**, *38*, 349.
(8) Koblenz, T. S.; Wassenaar, J.; Reek, J. N. H. *Chem. Soc. Rev.* **2008**, *37*, 247.
(9) Wiester, M. J.; Ulmann, P. A.; Mirkin, C. A. *Angew. Chem., Int. Ed.* **2011**, *50*, 114.
(10) Ballester, P. *Chem. Soc. Rev.* **2010**, *39*, 3810.
(11) Lehn, J. M. *Supramolecular Chemistry*: VCH: Weinheim, Germany, 1995.
(12) Conn, M. M.; Rebek, J., Jr. *Chem. Rev.* **1997**, *97*, 1647.
(13) Schmidtchen, F. P.; Berger, M. *Chem. Rev.* **1997**, *97*, 1609.
(14) Arunachalam, M.; Ravikumar, I.; Ghosh, P. *J. Org. Chem.* **2008**, *73*, 9144.
(15) Mateus, P.; Bernier, N.; Delgado, R. *Coord. Chem. Rev.* **2010**, *254*, 1726.
(16) Dietrich, B.; Lehn, J. M.; Sauvage, J. P. *Tetrahedron Lett.* **1969**, *10*, 2889.
(17) Simmons, H. E.; Park, C. H. *J. Am. Chem. Soc.* **1968**, *90*, 2428.
(18) Simmons, H. E.; Park, C. H. *J. Am. Chem. Soc.* **1968**, *90*, 2431.
(19) Kang, S.-O.; Llinares, J. M.; Day, V. W.; Bowman-James, K. *Chem. Soc. Rev.* **2010**, *39*, 3980.
(20) Saalfrank, R. W.; Dresel, A.; Seitz, V.; Trummer, S.; Hampel, F.; Teichert, M.; Stalke, D.; Stadler, C.; Daub, J.; Schunemann, V.; Trautwein, A. X. *Chem.—Eur. J.* **1997**, *3*, 2058.
(21) Saalfrank, R. W.; Seitz, V.; Caulder, D. L.; Raymond, K. N.; Teichert, M.; Stalke, D. *Eur. J. Inorg. Chem.* **1998**, 1313.
(22) Catalano, V. J.; Malwitz, M. A.; Noll, B. C. *Inorg. Chem.* **2002**, *41*, 6553.
(23) Catalano, V. J.; Bennett, B. L.; Malwitz, M. A.; Yson, R. L.; Kar, H. M.; Muratidis, S.; Horner, S. J. *Comments Inorg. Chem.* **2003**, *24*, 39.
(24) Amouri, H.; Rager, M. N.; Cagnol, F.; Vaissermann, J. *Angew. Chem., Int. Ed.* **2001**, *40*, 3636.
(25) Amouri, H.; Guyard-Duhayon, C.; Vaissermann, J.; Rager, M. N. *Inorg. Chem.* **2002**, *41*, 1397.
(26) Boyer, J. L.; Kuhlman, M. L.; Rauchfuss, T. B. *Acc. Chem. Res.* **2007**, *40*, 233.
(27) Boyer, J. L.; Yao, H.; Kuhlman, M. L.; Rauchfuss, T. B.; Wilson, S. *Eur. J. Inorg. Chem.* **2007**, 2721.
(28) Contakes, S. M.; Klausmeyer, K. K.; Milberg, R. M.; Wilson, S. R.; Rauchfuss, T. B. *Organometallics* **1998**, *17*, 3633.

(29) Kuhlman, M. L.; Yao, H.; Rauchfuss, T. B. *Chem. Commun.* **2004**, 1370.
(30) Kuhlman, M. L.; Rauchfuss, T. B. *Inorg. Chem.* **2004**, *43*, 430.
(31) Hsu, S. C. N.; Ramesh, M.; Espenson, J. H.; Rauchfuss, T. B. *Angew. Chem., Int. Ed.* **2003**, *42*, 2663.
(32) Kuhlman, M. L.; Rauchfuss, T. B. *J. Am. Chem. Soc.* **2003**, *125*, 10084.
(33) Severin, K. *Coord. Chem. Rev.* **2003**, *245*, 3.
(34) Severin, K. *Chem. Commun.* **2006**, 3859.
(35) Mirtschin, S.; Krasniqi, E.; Scopelliti, R.; Severin, K. *Inorg. Chem.* **2008**, *47*, 6375.
(36) Lehaire, M.-L.; Scopelliti, R.; Herdeis, L.; Polborn, K.; Mayer, P.; Severin, K. *Inorg. Chem.* **2004**, *43*, 1609.
(37) Mirtschin, S.; Slabon-Turski, A.; Scopelliti, R.; Velders, A. H.; Severin, K. *J. Am. Chem. Soc.* **2010**, *132*, 14004.
(38) Granzhan, A.; Riis-Johannessen, T.; Scopelliti, R.; Severin, K. *Angew. Chem., Int. Ed.* **2010**, *49*, 5515.
(39) Granzhan, A.; Schouwey, C.; Riis-Johannessen, T.; Scopelliti, R.; Severin, K. *J. Am. Chem. Soc.* **2011**, *133*, 7106.
(40) Yamanari, K.; Ito, R.; Yamamoto, S.; Fuyuhiro, A. *Chem. Commun.* **2001**, 1414.
(41) Lacour, J.; Ginglinger, C.; Grivet, C.; Bernardinelli, G. *Angew. Chem., Int. Ed.* **1997**, *36*, 608.
(42) Mimassi, L.; Guyard-Duhayon, C.; Rager, M. N.; Amouri, H. *Inorg. Chem.* **2004**, *43*, 6644.
(43) Mimassi, L.; Cordier, C.; Guyard-Duhayon, C.; Mann, B. E.; Amouri, H. *Organometallics* **2007**, *26*, 860.
(44) Therrien, B. *Eur. J. Inorg. Chem.* **2009**, 2445.
(45) Therrien, B. *J. Organomet. Chem.* **2011**, *696*, 637.
(46) Freudenreich, J.; Barry, N. P. E; Suess-Fink, G.; Therrien, B. *Eur. J. Inorg. Chem.* **2011**, 2400.
(47) Freudenreich, J.; Furrer, J.; Suss-Fink, G.; Therrien, B. *Organometallics* **2011**, *30*, 942.
(48) Barry, N. P. E; Therrien, B. *Eur. J. Inorg. Chem.* **2009**, 4695.
(49) Barry, N. P. E; Furrer, J.; Freudenreich, J.; Suess-Fink, G.; Therrien, B. *Eur. J. Inorg. Chem.* **2010**, 725.
(50) Barry, N. P. E; Furrer, J.; Therrien, B. *Helv. Chim. Acta* **2010**, *93*, 1313.
(51) Pitto-Barry, A.; Barry Nicolas, P. E.; Zava, O.; Deschenaux, R.; Therrien, B. *Chem. Asian. J.* **2011**, *6*, 1595.
(52) Pitto-Barry, A.; Barry, N. P. E; Zava, O.; Deschenaux, R.; Dyson, P. J.; Therrien, B. *Chem.—Eur. J.* **2011**, *17*, 1966.
(53) Han, Y. F.; Lin, Y. J.; Jia, W.-G.; Jin, G. X. *Dalton Trans.* **2009**, 2077.
(54) Han, Y. F.; Li, H.; Jin, G. X. *Chem. Commun.* **2010**, *46*, 6879.
(55) Han, Y. F.; Fei, Y.; Jin, G. X. *Dalton Trans.* **2010**, *39*, 3976.
(56) Wang, G.-L.; Lin, Y.-J.; Berke, H.; Jin, G.-X. *Inorg. Chem.* **2010**, *49*, 2193.
(57) Jia, W.-G.; Han, Y.-F.; Lin, Y.-J.; Weng, L.-H.; Jin, G.-X. *Organometallics* **2009**, *28*, 3459.
(58) Han, Y. F.; Jia, W.-G.; Lin, Y. J.; Jin, G. X. *Angew. Chem., Int. Ed.* **2009**, *48*, 6234.
(59) Yu, W.-B.; Han, Y.-F.; Lin, Y.-J.; Jin, G.-X. *Chem.—Eur. J.* **2011**, *17*, 1863.
(60) Hay, C.; Le Vilain, D.; Deborde, V.; Réau, R.; Toupet, L. *Chem. Commun.* **1999**, 345.
(61) Hay, C.; Hissler, M.; Fischmeister, C.; Rault-Berthelot, J.; Toupet, L.; Nyulaszi, L.; Réau, R. *Chem.—Eur. J.* **2001**, *7*, 4222.
(62) Leca, F.; Lescop, C.; Rodriguez-Sanz, E.; Costuas, K.; Halet, J.-F.; Réau, R. *Angew. Chem., Int. Ed.* **2005**, *44*, 4362.
(63) Nohra, B.; Rodriguez-Sanz, E.; Lescop, C.; Réau, R. *Chem.—Eur. J.* **2008**, *14*, 3391.
(64) Yao, Y.; Shen, W.; Nohra, B.; Lescop, C.; Réau, R. *Chem.—Eur. J.* **2010**, *16*, 7143.
(65) Kojima, T.; Inui, Y.; Miyazaki, S.; Shiro, M.; Fukuzumi, S. *Chem. Commun.* **2009**, 6643.
(66) Moussa, J.; Gandon, V.; Rager, M. N.; Malacria, M.; Chamoreau, L.-M.; Amouri, H. *Eur. J. Inorg. Chem.* **2009**, 3703.
(67) Bondi, A. *J. Phys. Chem.* **1964**, *68*, 441.
(68) Amouri, H.; Moussa, J.; Malacria, M.; Gandon, V. *Cryst. Growth Des.* **2009**, *9*, 5304.
(69) Gale, P. A. *Acc. Chem. Res.* **2011**, *44*, 216.
(70) Gimeno, N.; Vilar, R. *Coord. Chem. Rev.* **2006**, *250*, 3161.
(71) Mullen, K. M.; Beer, P. D. *Chem. Soc. Rev.* **2009**, *38*, 1701.
(72) Metrangolo, P.; Pilati, T.; Terraneo, G.; Biella, S.; Resnati, G. *CrystEngComm.* **2009**, *11*, 1187.
(73) Mercer, D. J.; Loeb, S. J. *Chem. Soc. Rev.* **2010**, *39*, 3612.
(74) Steed, J. W. *Chem. Soc. Rev.* **2009**, *38*, 506.
(75) Beer, P. D.; Bayly, S. R. *Anion Sensing* **2005**, *255*, 125.
(76) Teo, P.; Hor, T. S. A. *Coord. Chem. Rev.* **2011**, *255*, 273.
(77) Vilar, R. *Eur. J. Inorg. Chem.* **2008**, 357.
(78) Raehm, L.; Mimassi, L.; Guyard-Duhayon, C.; Amouri, H.; Rager, M. N. *Inorg. Chem.* **2003**, *42*, 5654.
(79) Mimassi, L.; Guyard-Duhayon, C.; Raehm, L.; Amouri, H. *Eur. J. Inorg. Chem.* **2002**, 2453.
(80) Beer, P. D.; Sambrook, M. R.; Curiel, D. *Chem. Commun.* **2006**, 2105.
(81) Diaz, P.; Benet-Buchholz, J.; Vilar, R.; White, A. J. P. *Inorg. Chem.* **2006**, *45*, 1617.
(82) Semeril, D.; Matt, D.; Harrowfield, J.; Schultheiss, N.; Toupet, L. *Dalton Trans.* **2009**, 6296.
(83) Dry, E. F. V.; Clegg, J. K.; Breiner, B.; Whitaker, D. E.; Stefak, R.; Nitschke, J. R. *Chem. Commun.* **2011**, *47*, 6021.
(84) Li, C.; Pattacini, R.; Graff, R.; Braunstein, P. *Angew. Chem., Int. Ed.* **2008**, *47*, 6856.
(85) Su, C. Y.; Cai, Y. P.; Chen, C. L.; Zhang, H. X.; Kang, B. S. *J. Chem. Soc., Dalton Trans.* **2001**, 359.
(86) Sun, W. Y.; Fan, J.; Okamura, T.; Xie, J.; Yu, K. B.; Ueyama, N. *Chem.—Eur. J.* **2001**, *7*, 2557.
(87) Liu, H. K.; Hu, J.; Wang, T. W.; Yu, X. L.; Liu, J.; Kang, B. S. *J. Chem. Soc., Dalton Trans.* **2001**, 3534.
(88) Su, C. Y.; Cai, Y. P.; Chen, C. L.; Lissner, F.; Kang, B. S.; Kaim, W. *Angew. Chem., Int. Ed.* **2002**, *41*, 3371.
(89) Fan, J.; Zhu, H. F.; Okamura, T.; Sun, W. Y.; Tang, W. X.; Ueyama, N. *Chem.—Eur. J.* **2003**, *9*, 4724.
(90) Liu, H. K.; Huang, X. H.; Lu, T.; Wang, X.; Sun, W. Y.; Kang, B. S. *Dalton Trans.* **2008**, 3178.
(91) Wenzel, M.; Bruere, S. R.; Knapp, Q. W.; Tasker, P. A.; Plieger, P. G. *Dalton Trans.* **2010**, *39*, 2936.
(92) McMorran, D. A.; Steel, P. J. *Angew. Chem., Int. Ed.* **1998**, *37*, 3295.
(93) Amouri, H.; Mimassi, L.; Rager, M. N.; Mann, B. E.; Guyard-Duhayon, C.; Raehm, L. *Angew. Chem., Int. Ed.* **2005**, *44*, 4543.
(94) Amouri, H.; Desmarets, C.; Bettoschi, A.; Rager, M. N.; Boubekeur, K.; Rabu, P.; Drillon, M. *Chem.—Eur. J.* **2007**, *13*, 5401.
(95) Campos-Fernandez, C. S.; Schottel, B. L.; Chifotides, H. T.; Bera, J. K.; Bacsa, J.; Koomen, J. M.; Russell, D. H.; Dunbar, K. R. *J. Am. Chem. Soc.* **2005**, *127*, 12909.
(96) Manzano, B. R.; Jalon, F. A.; Ortiz, M. I.; Soriano, M. L.; de la Torre, F. G.; Elguero, J.; Maestro, M. A.; Mereiter, K.; Claridge, T. D. W. *Inorg. Chem.* **2008**, *47*, 413.
(97) Suen, M.-C.; Yeh, C.-W.; Ho, Y.-W.; Wang, J.-C. *New J. Chem.* **2009**, *33*, 2419.
(98) Desmarets, C.; Poli, F.; Le Goff, X. F.; Muller, K.; Amouri, H. *Dalton Trans.* **2009**, 10429.
(99) Wu, B.; Yuan, D.; Lou, B.; Han, L.; Liu, C.; Zhang, C.; Hong, M. *Inorg. Chem.* **2005**, *44*, 9175.
(100) Barbour, L. J.; Orr, G. W.; Atwood, J. L. *Nature* **1998**, *393*, 671.
(101) Desmarets, C.; Policar, C.; Chamoreau, L. M.; Amouri, H. *Eur. J. Inorg. Chem.* **2009**, 4396.
(102) Liu, H. K.; Cai, Y.; Luo, W. P.; Tong, F. Y.; You, C. X.; Lu, S. H.; Huang, X. H.; Ye, H. Y.; Su, F.; Wang, X. J. *Inorg. Chem. Commun.* **2009**, *12*, 457.
(103) Kim, K. H.; Park, J. S.; Kang, T. Y.; Oh, K.; Seo, M. S.; Sohn, Y. S.; Jun, M. J.; Nam, W.; Kim, K. M. *Chem.—Eur. J.* **2006**, *12*, 7078.

(104) Wyler, R.; de Mendoza, J.; Rebek, J. *Angew. Chem., Int. Ed.* **1993**, *32*, 1699.
(105) Mann, S.; Huttner, G.; Zsolnai, L.; Heinze, K. *Angew. Chem., Int. Ed.* **1996**, *35*, 2808.
(106) Glasson, C. R. K.; Meehan, G. V.; Clegg, J. K.; Lindoy, L. F.; Turner, P.; Duriska, M. B.; Willis, R. *Chem. Commun.* **2008**, 1190.
(107) Glasson, C. R. K.; Clegg, J. K.; McMurtrie, J. C.; Meehan, G. V.; Lindoy, L. F.; Motti, C. A.; Moubaraki, B.; Murray, K. S.; Cashion, J. D. *Chem. Sci.* **2011**, *2*, 540.
(108) Fleming, J. S.; Mann, K. L. V.; Carraz, C. A.; Psillakis, E.; Jeffery, J. C.; McCleverty, J. A.; Ward, M. D. *Angew. Chem., Int. Ed.* **1998**, *37*, 1279.
(109) Paul, R. L.; Bell, Z. R.; Fleming, J. S.; Jeffery, J. C.; McCleverty, J. A.; Ward, M. D. *Heteroat. Chem.* **2002**, *13*, 567.
(110) Paul, R. L.; Bell, Z. R.; Jeffery, J. C.; McCleverty, J. A.; Ward, M. D. *Proc. Natl. Acad. Sci. U. S. A.* **2002**, *99*, 4883.
(111) Tidmarsh, I. S.; Taylor, B. F.; Hardie, M. J.; Russo, L.; Clegg, W.; Ward, M. D. *New. J. Chem.* **2009**, *33*, 366.
(112) Argent, S. P.; Riis-Johannessen, T.; Jeffery, J. C.; Harding, L. P.; Ward, M. D. *Chem. Commun.* **2005**, 4647.
(113) Argent, S. P.; Adams, H.; Harding, L. P.; Ward, M. D. *Dalton Trans.* **2006**, 542.
(114) Paul, R. L.; Argent, S. P.; Jeffery, J. C.; Harding, L. P.; Lynam, J. M.; Ward, M. D. *Dalton Trans.* **2004**, 3453.
(115) Bell, Z. R.; Harding, L. P.; Ward, M. D. *Chem. Commun.* **2003**, 2432.
(116) Bell, Z. R.; Jeffery, J. C.; McCleverty, J. A.; Ward, M. D. *Angew. Chem., Int. Ed.* **2002**, *41*, 2515.
(117) Argent, S. P.; Adams, H.; Riis-Johannessen, T.; Jeffery, J. C.; Harding, L. P.; Ward, M. D. *J. Am. Chem. Soc.* **2006**, *128*, 72.
(118) Custelcean, R.; Bosano, J.; Bonnesen, P. V.; Kertesz, V.; Hay, B. P. *Angew. Chem., Int. Ed.* **2009**, *48*, 4025.
(119) Mal, P.; Breiner, B.; Rissanen, K.; Nitschke, J. R. *Science* **2009**, *324*, 1697.
(120) Meng, W. J.; Breiner, B.; Rissanen, K.; Thoburn, J. D.; Clegg, J. K.; Nitschke, J. R. *Angew. Chem., Int. Ed.* **2011**, *50*, 3479.
(121) Seidel, S. R.; Stang, P. J. *Acc. Chem. Res.* **2002**, *35*, 972.
(122) Zheng, Y. R.; Zhao, Z.; Wang, M.; Ghosh, K.; Pollock, J. B.; Cook, T. R.; Stang, P. J. *J. Am. Chem. Soc.* **2010**, *132*, 16873.
(123) Wang, M.; Zheng, Y.-R.; Ghosh, K.; Stang, P. J. *J. Am. Chem. Soc.* **2010**, *132*, 6282.
(124) Fujita, M.; Tominaga, M.; Hori, A.; Therrien, B. *Acc. Chem. Res.* **2005**, *38*, 369.
(125) Fujita, M.; Umemoto, K.; Yoshizawa, M.; Fujita, N.; Kusukawa, T.; Biradha, K. *Chem. Commun.* **2001**, 509.
(126) Kusukawa, T.; Fujita, M. *J. Am. Chem. Soc.* **2002**, *124*, 13576.
(127) Yu, S. Y.; Kusukawa, T.; Biradha, K.; Fujita, M. *J. Am. Chem. Soc.* **2000**, *122*, 2665.
(128) Fujita, M.; Su, S.-Y.; Kusukawa, T.; Funaki, H.; Ogura, K.; Yamaguchi, K. *Angew. Chem., Int. Ed.* **1998**, *37*, 2082.
(129) Sun, W. Y.; Kusukawa, T.; Fujita, M. *J. Am. Chem. Soc.* **2002**, *124*, 11570.
(130) Nakabayashi, K.; Kawano, M.; Kato, T.; Furukawa, K.; Ohkoshi, S.; Hozumi, T.; Fujita, M. *Chem. Asian. J.* **2007**, *2*, 164.
(131) Nakabayashi, K.; Kawano, M.; Fujita, M. *Angew. Chem., Int. Ed.* **2005**, *44*, 5322.
(132) Nakabayashi, K.; Kawano, M.; Yoshizawa, M.; Ohkoshi, S.; Fujita, M. *J. Am. Chem. Soc.* **2004**, *126*, 16694.
(133) Inokuma, Y.; Kawano, M.; Fujita, M. *Nat. Chem.* **2011**, *3*, 349.
(134) Yoshizawa, M.; Kusukawa, T.; Fujita, M.; Sakamoto, S.; Yamaguchi, K. *J. Am. Chem. Soc.* **2001**, *123*, 10454.
(135) Yoshizawa, M.; Kusukawa, T.; Fujita, M.; Yamaguchi, K. *J. Am. Chem. Soc.* **2000**, *122*, 6311.
(136) Kawano, M.; Kobayashi, Y.; Ozeki, T.; Fujita, M. *J. Am. Chem. Soc.* **2006**, *128*, 6558.
(137) Inokuma, Y.; Yoshioka, S.; Fujita, M. *Angew. Chem., Int. Ed.* **2010**, *49*, 8912.
(138) Yoshizawa, M.; Klosterman, J. K.; Fujita, M. *Angew. Chem., Int. Ed.* **2009**, *48*, 3418.
(139) Murase, T.; Fujita, M. *Chem. Rec.* **2010**, *10*, 342.
(140) Yoshizawa, M.; Tamura, M.; Fujita, M. *Science* **2006**, *312*, 251.
(141) Kusukawa, T.; Nakai, T.; Okano, T.; Fujita, M. *Chem. Lett.* **2003**, *32*, 284.
(142) Murase, T.; Horiuchi, S.; Fujita, M. *J. Am. Chem. Soc.* **2010**, *132*, 2866.
(143) Furusawa, T.; Kawano, M.; Fujita, M. *Angew. Chem., Int. Ed.* **2007**, *46*, 5717.
(144) Yamaguchi, T.; Fujita, M. *Angew. Chem., Int. Ed.* **2008**, *47*, 2067.
(145) Murase, T.; Peschard, S.; Horiuchi, S.; Nishioka, Y.; Fujita, M. *Supramol. Chem.* **2011**, *23*, 199.
(146) Nishioka, Y.; Yamaguchi, T.; Kawano, M.; Fujita, M. *J. Am. Chem. Soc.* **2008**, *130*, 8160.
(147) Ito, H.; Kusukawa, T.; Fujita, M. *Chem. Lett.* **2000**, 598.
(148) Yoshizawa, M.; Sato, N.; Fujita, M. *Chem. Lett.* **2005**, *34*, 1392.
(149) Caulder, D. L.; Powers, R. E.; Parac, T. N.; Raymond, K. N. *Angew. Chem., Int. Ed.* **1998**, *37*, 1840.
(150) Scherer, M.; Caulder, D. L.; Johnson, D. W.; Raymond, K. N. *Angew. Chem., Int. Ed.* **1999**, *38*, 1588.
(151) Johnson, D. W.; Raymond, K. N. *Inorg. Chem.* **2001**, *40*, 5157.
(152) Albrecht, M.; Burk, S.; Weis, P. *Synthesis* **2008**, 2963.
(153) Albrecht, M.; Stockel, B. A. *Synlett* **2011**, 121.
(154) Liu, T. F.; Liu, Y.; Xuan, W. M.; Cui, Y. *Angew. Chem., Int. Ed.* **2010**, *49*, 4121.
(155) Xi, X.; Fang, Y.; Dong, T.; Cui, Y. *Angew. Chem., Int. Ed.* **2011**, *50*, 1154.
(156) Fiedler, D.; Pagliero, D.; Brumaghim, J. L.; Bergman, R. G.; Raymond, K. N. *Inorg. Chem.* **2004**, *43*, 846.
(157) Fiedler, D.; Leung, D. H.; Bergman, R. G.; Raymond, K. N. *J. Am. Chem. Soc.* **2004**, *126*, 3674.
(158) Nuckolls, C.; Hof, F.; Martin, T.; Rebek, J., Jr. *J. Am. Chem. Soc.* **1999**, *121*, 10281.
(159) Leung, D. H.; Fiedler, D.; Bergman, R. G.; Raymond, K. N. *Angew. Chem., Int. Ed.* **2004**, *43*, 963.
(160) Leung, D. H.; Bergman, R. G.; Raymond, K. N. *J. Am. Chem. Soc.* **2006**, *128*, 9781.
(161) Fiedler, D.; Bergman, R. G.; Raymond, K. N. *Angew. Chem., Int. Ed.* **2004**, *43*, 6748.
(162) Brown, C. J.; Bergman, R. G.; Raymond, K. N. *J. Am. Chem. Soc.* **2009**, *131*, 17530.
(163) Pluth, M. D.; Bergman, R. G.; Raymond, K. N. *Science* **2007**, *316*, 85.
(164) Pluth, M. D.; Bergman, R., G.; Raymond, K., N. *Angew. Chem., Int. Ed.* **2007**, *46*, 8587.
(165) Hastings, C. J.; Pluth, M. D.; Bergman, R. G.; Raymond, K. N. *J. Am. Chem. Soc.* **2010**, *132*, 6938.
(166) Wang, Z. J.; Brown, C. J.; Bergman, R. G.; Raymond, K. N.; Toste, F. D. *J. Am. Chem. Soc.* **2011**, *133*, 7358.
(167) Merlau, M. L.; Del Pilar Mejia, M.; Nguyen, S. T.; Hupp, J. T. *Angew. Chem., Int. Ed.* **2001**, *40*, 4239.
(168) Lee, S. J.; Mulfort, K. L.; Zuo, X.; Goshe, A. J.; Wesson, P. J.; Nguyen, S. T.; Hupp, J. T.; Tiede, D. M. *J. Am. Chem. Soc.* **2008**, *130*, 836.
(169) Lee, S. J.; Cho, S.-H.; Mulfort, K. L.; Tiede, D. M.; Hupp, J. T.; Nguyen, S. T. *J. Am. Chem. Soc.* **2008**, *130*, 16828.
(170) Gianneschi, N. C.; Bertin, P. A.; Nguyen, S. T.; Mirkin, C. A.; Zakharov, L. N.; Rheingold, A. L. *J. Am. Chem. Soc.* **2003**, *125*, 10508.
(171) Masar, M. S., III; Gianneschi, N. C.; Oliveri, C. G.; Stern, C. L.; Nguyen, S. T.; Mirkin, C. A. *J. Am. Chem. Soc.* **2007**, *129*, 10149.
(172) Oliveri, C. G.; Gianneschi, N. C.; Nguyen, S. T.; Mirkin, C. A.; Stern, C. L.; Wawrzak, Z.; Pink, M. *J. Am. Chem. Soc.* **2006**, *128*, 16286.
(173) Yoon, H. J.; Heo, J.; Mirkin, C. A. *J. Am. Chem. Soc.* **2007**, *129*, 14182.
(174) Gianneschi, N. C.; Cho, S.-H.; Nguyen, S. T.; Mirkin, C. A. *Angew. Chem., Int. Ed.* **2004**, *43*, 5503.
(175) Slagt, V. F.; Reek, J. N. H.; Kamer, P. C. J.; Van Leeuwen, P. W. N. M. *Angew. Chem., Int. Ed.* **2001**, *40*, 4271.

(176) Kleij, A. W.; Reek, J. N. H. *Chem.—Eur. J.* **2006**, *12*, 4218.
(177) Kleij, A. W.; Lutz, M.; Spek, A. L.; van Leeuwen, P. W. N. M.; Reek, J. N. H. *Chem. Commun.* **2005**, 3661.
(178) Kuil, M.; Soltner, T.; Van Leeuwen, P. W. N. M.; Reek, J. N. H. *J. Am. Chem. Soc.* **2006**, *128*, 11344.
(179) Bellini, R.; Chikkali, S. H.; Berthon-Gelloz, G.; Reek, J. N. H. *Angew. Chem., Int. Ed.* **2011**, *50*, 7342.
(180) Oisaki, K.; Li, Q. W.; Furukawa, H.; Czaja, A. U.; Yaghi, O. M. *J. Am. Chem. Soc.* **2010**, *132*, 9262.
(181) Blake, A. J.; Champness, N. R.; Easun, T. L.; Allan, D. R.; Nowell, H.; George, M. W.; Jia, J.; Sun, X.-Z. *Nat. Chem.* **2010**, *2*, 688.